Inducing differences in modification degree and binding mode of organophosphonic acid grafted titania by changing pH and hydrocarbon chain length

An, R; Quinones, LC; Gys, N; DERVEAUX, Elien; Baert, K; Hauffman, T; ADRIAENSENS, Peter; Blockhuys, F & Meynen, V (2023) Inducing differences in modification degree and binding mode of organophosphonic acid grafted titania by changing pH and hydrocarbon chain length. In: APPLIED SURFACE SCIENCE, 639 (Art N° 158179).

DOI: 10.1016/j.apsusc.2023.158179
Handle: http://hdl.handle.net/1942/43163

Inducing differences in modification degree and binding mode of organophosphonic acid grafted titania by changing pH and hydrocarbon chain length

Rui An[1], Lourdes Chukiwanka Quiñones[1,a], Nick Gys[1,2,b], Elien Derveaux[3], Kitty Baert[4], Tom Hauffman[4], Peter Adriaensens[3], Frank Blockhuys[5], Vera Meynen[1,2,*]

[1]Laboratory of Adsorption and Catalysis (LADCA), Department of Chemistry, University of Antwerp, Universiteitsplein 1, 2610 Wilrijk, Belgium.

[2]Sustainable Materials, Flemish Institute for Technological Research (VITO NV), Boeretang 200, 2400 Mol, Belgium.

[3]Analytical and Circular Chemistry (ACC), Institute for Materials Research (IMO), Hasselt University, Agoralaan 1, 3590 Diepenbeek, Belgium

[4]Research Group Electrochemical and Surface Engineering (SURF), Department Materials and Chemistry, Vrije Universiteit Brussel, Pleinlaan 2, 1050 Brussel, Belgium.

[5]Structural Chemistry Group, Department of Chemistry, University of Antwerp, Groenenborgerlaan 171, 2020 Antwerpen, Belgium.

[*]Corresponding author: vera.meynen@uantwerpen.be

[a]Present address: Umicore NV, Watertorenstraat 33, 2250 Olen, Belgium.

[b]Present addresses: Centre for Membrane Separations, Adsorption, Catalysis and Spectroscopy (cMACS), KU Leuven, Celestijnenlaan 200F, 3001 Leuven, Belgium; Research Group Electrochemical and Surface Engineering (SURF), Vrije Universiteit Brussel, Pleinlaan 2, 1050 Brussels, Belgium.

Abstract

Organically modified metal oxide surfaces are of interest in many applications since they combine the advantages of metal oxide supports (structural properties, chemical and mechanical stability) and organic functionalities (for specific surface interactions). Although surface modification with organophosphonic acids (PAs) with an alkyl or aminoalkyl functional group on TiO_2 has been investigated previously, knowledge of the synthesis-properties correlation (e.g. the binding mode of the PAs) is still lacking, especially for functional group-surface interactions. These are however important as they can influence functional group availability in applications such as (metal) sorption. In this work, the dependence of modification degree and phosphorus chemical environment on pH and chain length (C1 to C6) was investigated with TGA, ICP-OES, nitrogen/argon sorption, XPS, and solid-state ^{31}P-NMR and DFT calculations. The TGA and the ICP-OES results showed a clear impact of pH on surface modification degrees, with a different response for modification with alkyl- and aminoalkylphosphonic acids, featuring a more rapid decrease in modification degrees from pH 2 upwards for the alkylphosphonic acids compared to the aminoalkylphosphonic acids. Moreover, a clear correlation can be found between the aminoalkyl chain length and the NH_2/NH_3^+ ratio. In addition, a positive correlation between the modification degree and the protonation degree of the amine group is observed for aminomethylphosphonic acid (AMPA) and 2-aminoethylphosphonic acid (2AEPA) modified samples, while this is absent for longer alkyl chains. This is supported by DFT calculations that indicate that the most stable binding modes of AMPA and 2AEPA grafted on the anatase (101) surface include hydrogen bonds between NH_3^+ and the surface oxygen atoms, in contrast, the

most stable binding modes for 3-aminopropylphosphonic acid (3APPA), 4-aminobutylphosphonic acid (4ABPA), and 6-aminohexylphosphonic acid (6AHPA) grafted on the anatase (101) surface involve a Lewis acid-base interaction between NH_2 and a surface Ti site.

Keywords

TiO_2 surface modification**,** (amino)alkylphosphonic acids, hydrocarbon chain length, pH, NH_2/NH_3^+ ratio

1. Introduction

Metal oxide supports such as titania have found their way into a wide range of applications such as separation technologies [1]–[5], solar cells [6], [7], chemical sensors [8], catalysis [9], [10] and pharmaceuticals [11], [12]. In addition to their structural properties, high mechanical and chemical stability, the surfaces of metal oxides can be functionalized with organic groups in order to introduce specific surface interactions, adjusting their applicability and performance. One of the methods for surface functionalization is the modification with organophosphonic acids (PAs) or their derivatives, which are widely used precursors to introduce organic functional groups to titania surfaces [13]–[20]. PA-modified materials are applied in many fields such as membranes [3], [4], [21], chromatography [22]–[24], and photoelectric devices [25]. PAs graft to the titania surface via a condensation reaction between the P-OH group of the PAs and the surface hydroxyl groups, while the phosphoryl oxygen (P=O) coordinates with

Lewis acid sites on titania [26], resulting in different binding modes, e.g. mono-, bi-, and tridentate [26], [27].

In the process of synthesizing PA-modified materials, many reaction conditions including solvent, temperature, pH, and reaction time could influence the modified surface and thus it is vital to have knowledge on synthesis - properties correlations in order to obtain desired surface properties for targeted applications. Chen and co-workers investigated the influence of the solvent on the surface modification of indium tin oxides and the structure of the formed monolayer [28]. They discovered that the solvent is a key factor in the quality of the grafted organic layer. Modification in solvents with high dielectric constants such as water and DMSO leads to disordered monolayers because of the strong polar interaction between the solvent and the surface. They found that only the solvents with almost no interaction with the surface could result in the formation of highly ordered monolayers. The influence of the solvent on the modification of titania with PAs was also confirmed by Roevens and co-workers [19], [20]. They concluded that modification in water results in the formation of "islands" of grafted propylphosphonic acid (PPA) on the surface while modification in toluene leads to a random homogeneous distribution of PPA molecules on the surface. They also suggested that these differences could originate from the competing interactions of the solvent and the PPA molecules at the surface. In the case of water as the solvent, the PPA molecules and water compete for adsorption on the surface. It was proposed that upon displacement of water molecules from the surface by PPA molecules and bonding of the PPA molecules to the surface, the water molecules exhibit less tendency to adsorb among the hydrophobic propyl chains.

Therefore, it is likely that these chains interact more with each other, leading to a self-assembly process that results in the formation of patches of grafted PPA molecules on the surface. As a result, “islands” of local self-organization on the surface were created next to the patches of hydrophilic nests. In contrast, no such competition exists in toluene and thus no “islands” could be formed. Instead, a more homogeneous and randomly distributed layer of PPA molecules was formed on the surface. Water sorption isotherms and butanol displacement microcalorimetry also correlated these differences induced by the solvent to the variation in interaction energy with water and the hydrophobic character of the modified materials [20]. Furthermore, Roevens and co-workers also found that a higher temperature (130 °C vs. 90 °C) can promote the formation of titanium propylphosphonates in water while no obvious impact of temperature was found when working in toluene [19].

The use of water as the solvent in the surface modification of metal oxides with PAs is of particular interest since water is environmentally friendly compared to organic solvents. In water, the pH could play an important role in surface modification. The surface hydroxyl groups of the metal oxides could behave as base or acid as a function of pH (M-OH + H^+ ⇌ MOH_2^+ and M-OH ⇌ MO^- + H^+), while altering surface charge, and the pH at which the surface is electrically neutral is the isoelectric point (IEP) [29]. Moreover, Schafer et al. [30] and Gao et al. [14] described a dissolution-precipitation process at the surface of zirconia, responsible for metal phosphonate formation, which is promoted under harsh grafting conditions such as low pH (< 2), high concentration of PA (0.1 M), high temperature (100 °C), and long reaction times (7 days). Guerrero et al. also observed this side reaction on titania, forming a titanium

phenylphosphonate layer at elevated temperature (120 °C) [15]. Roevens et al. also reported the formation of titanium propylphosphonate with a combination of low pH (2.1 - 2.5), high temperature (130 °C), and high concentration of propylphosphonic acid (0.15 M) in 4 hours reaction time [19]. Queffèlec et al. suggested varying the pH of the aqueous alkylphosphonic acid solution, the use of organic solvents or the ester of the phosphonic acid in order to solely obtain monolayer grafting [31]. Veclani et al. performed DFTB calculations and suggested that the formation of di-anionic acid species, resulting from either a proton transfer process or a variation in pH, favors the anchoring of alkylphosphonic acid to rutile TiO_2 (110) [32]. Nevertheless, the influence of pH on surface modification has not yet been studied systematically for alkyl and aminoalkyl functional groups on titania with respect to the modification degree and interaction of the functional group with the surface. It is a crucial missing piece of knowledge for controlling the surface properties of the modified material, particularly when the phosphonate moiety and the amine group are able to (de)protonate.

The amine group in PAs modified titania introduces and expands the range of specific interactions in applications such as CO_2 capture, rare earth element recovery, and Pd adsorption [33]–[38]. Tudisco et al. [39], Canepa et al. [36], and Gys et al. [37] found the presence of both free NH_2 and protonated NH_3^+ groups on aminoalkylphosphonic acid grafted Fe_3O_4 and TiO_2 surfaces. Gys and co-workers further found that the hydrocarbon chain length of aminoalkylphosphonic acids with terminal amine functionalities had an impact on the protonation degree of the amine group of surface-grafted materials and the folding back of the amine groups towards the surface [37], [38]. However, the underlying reason for the

protonation degree of the amine groups and a deeper understanding of the correlation between the hydrocarbon chain length and the bending back of the amine groups is still missing. Hence, this article aims to elucidate the underlying reason for the impact of the chain length on the chemical state(s) of the amine group and its correlation to the interaction of the PAs with the surface, as well as the binding mode of the PAs. In addition, the influence of pH on the interaction of PAs with the surface and its impact on the surface properties are explored with alkylphosphonic acids and aminoalkylphosphonic acids with varying chain lengths.

2. Material and methods

TiO_2 P25 was purchased from Sigma-Aldrich (catalog number: 718467-100G, ≥ 99.5 %) and used without pretreatment. P25 consists of ~83 % anatase, ~13 % rutile, and ~4 % amorphous fraction as characterized by electron energy loss spectroscopy (EELS) [40]. A BET (Brunauer-Emmett-Teller) surface area of 51 m^2/g was obtained with nitrogen sorption at -196 °C using a Quantachrome Quadrasorb automated sorption system. The average primary particle size of P25 is approximately 21 nm according to the information provided by the supplier.

Nine organophosphonic acids were used in this research (the structural formulas are listed in Figure 1). Methylphosphonic acid (MPA, ≥ 98 %), hexylphosphonic acid (HPA, 95 %), and 2-aminoethylphosphonic (2AEPA, 99 %) were purchased from Sigma-Aldrich. Propylphosphonic acid (PPA, ≥ 98 %) was purchased from Cayman Chemical Company. Butylphosphonic acid (BPA, 98 %) and aminomethylphosphonic acid (AMPA, 99 %) were

purchased from Alfa Aesar. 3-Aminopropylphosphonic acid (3APPA, 98 %) and 4-aminobutylphosphonic acid (4ABPA, 95 %) were purchased from abcr GmbH. Finally, 6-aminohexylphosphonic acid (6AHPA, ≥ 98 %) hydrochloride salt was purchased from SiKÉMIA. They were used in synthesis without pretreatment.

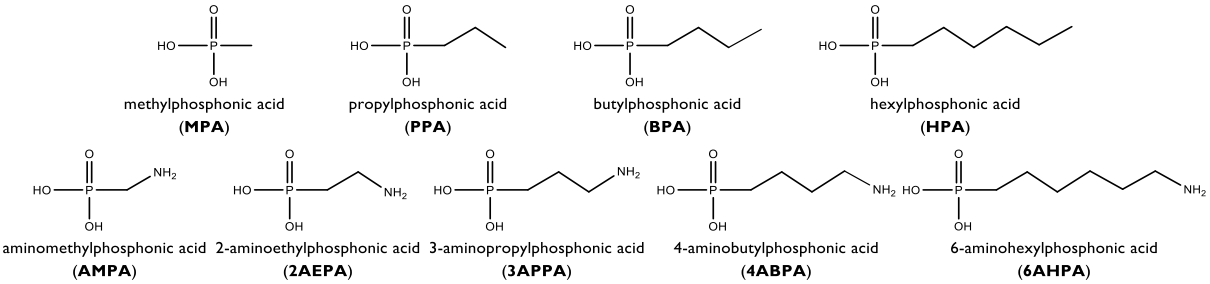

Figure 1. The structural formulas of the organophosphonic acids used in this work.

2.1 Surface modification with organophosphonic acid on P25

One gram of P25 was stirred for 4 h in a 20 mL heated (90 °C) aqueous organophosphonic acid (PA) solution with a concentration between 4 and 100 mM. The pH of the PA solutions was adjusted to 2, 3, 4, 6, 8, and 10 prior to the addition of the P25 by means of a 1 M HCl solution, or a 2 M NaOH solution. After modification, the samples were washed by centrifugation (5000 rpm) with 3 times 30 mL of water. After the washing procedure, the samples were dried overnight in an oven at 60°C. Finally, the samples were sealed inside a glovebox under Ar and then stored in a dry desiccator which was kept in darkness to prevent degradation [41].

The samples were labeled with a systematic name: the first part represents the phosphonic acid used for surface modification (MPA/PPA/BPA/HPA/AMPA/2AEPA/3APPA/4ABPA/6AHPA), the second part represents the PA concentration (in mM) used for surface modification, and the

last part represents the pH of the PA solution. For example, MPA25pH8 is the sample modified in water using methylphosphonic acid with a concentration of 25 mM and in which the pH of the MPA solution was adjusted to 8.

2.2 Instrumentation

Nitrogen sorption measurements were performed at -196 °C on a Quantachrome Quadrasorb SI automated gas sorption system. Argon sorption measurements were performed at -186 °C on a Quantachrome AUTOSORB-1-MP automated gas sorption system. Prior to the measurements, the samples were degassed for 16 hours under a vacuum of around 0.02 mbar at 60 °C. The specific surface area and the C value were calculated using the Brunauer-Emmett-Teller (BET) method in the relative pressure range of 0.05 - 0.35.

Thermogravimetric analysis (TGA) was performed on a Mettler Toledo TGA/DSC 3+. The measurements were carried out in a continuous oxygen or argon flow of 80 mL/min and the samples were heated from 30 to 600 °C (for measurements in oxygen flow) or 1000 °C (for measurements in argon flow) with a heating rate of 10 °C/min. The modification degree expressed as the number of grafted groups per nm² (#groups/nm²) was calculated from the weight loss due to the burned or lost carbon groups (for all the samples apart from the MPA samples) by using the following formula:

$$\text{mod. deg.}\,(\text{groups}/\text{nm}^2) = \frac{N_A \times wt\%(R)}{S_{BET} \times MM(R) \times 100}$$

in which N_A is the Avogadro's constant (6.022×10^{23} mol^{-1}), wt%(R) is the weight loss

percentage of the organic group, MM(R) is the molar mass of the organic group (in g/mol), and S_{BET} is the BET specific surface area of the unmodified TiO_2 P25 (51×10^{18} nm^2/g). The experimental error is estimated to be 0.1 groups/nm² based on three repeated modifications with the same synthesis conditions.

Inductively Coupled Plasma Optical Emission Spectroscopy (ICP-OES) was performed on an Agilent Technologies 5100 ICP-OES to determine the modification degree of the MPA-modified samples by detecting the phosphorus content. Samples of 50 mg were digested in a solution of 1.5 mL HNO_3 (67 - 69 %), 1.5 mL HF (48 %), and 3.0 mL H_2SO_4 (96 %) for 24 hours at 250 °C. To neutralize the HF after digestion, 16 mL H_3BO_3 (4 %) was added. The modification degree was calculated from the weight percentage of phosphorus using the following formula:

$$\text{mod. deg.}\,(\text{groups}/\text{nm}^2) = \frac{N_A \times wt\%(P)}{S_{BET} \times MM(P) \times 100}$$

in which N_A is Avogadro's constant (6.022×10^{23} mol^{-1}), wt%(P) is the weight percentage of the phosphorus, MM (P) is the molar mass of the phosphorus (30.97 g/mol), and S_{BET} is the BET specific surface area of the unmodified TiO_2 P25 (51×10^{18} nm^2/g). The experimental error is estimated to be 0.1 groups/nm² based on three repeated modifications with the same synthesis conditions.

Phosphorus-31 solid-state Magic Angle Spinning Nuclear Magnetic Resonance (^{31}P MAS NMR) spectra were acquired at room temperature on an Agilent VNMRS DirectDrive 400 MHz spectrometer (9.4 T wide bore magnet) equipped with a T3HX 3.2 mm VT probe

dedicated for small sample volumes and high decoupling powers. Magic angle spinning was performed at 15 kHz using ceramic zirconia rotors of 3.2 mm in diameter (22 µL rotors). Other acquisition parameters were: a spectral width of 60 kHz, a 90° pulse length of 3.2 µs, a recycle delay time of 20 s, and between 2000-4000 accumulations. The ^{31}P MAS NMR measurements were performed on all modified TiO_2 P25 samples as well as on the pure AMPA, 2AEPA, and 3APPA precursors used for surface grafting. The applied acquisition time was 15 ms for the modified TiO_2 P25 samples, while for the PA precursors (AMPA, 2AEPA, and 3APPA) a 25 ms acquisition time was applied. High power proton dipolar decoupling during the acquisition time was set at 80 kHz. The phosphorus chemical shift scale was calibrated to orthophosphoric acid (H_3PO_4) at 0 ppm.

Phosphorus-31 solid-state Cross Polarization/Magic Angle Spinning Nuclear Magnetic Resonance (^{31}P CP/MAS NMR) spectra were acquired at room temperature on the same spectrometer using the same T3HX 3.2 mm probe and spinning speed as the ^{31}P MAS NMR measurements. Other acquisition parameters were: a spectral width of 60 kHz, a 90° pulse length of 3.1 µs, a spin-lock field for CP of 80 kHz, a contact time for CP of 1 ms, an acquisition time of 25 ms, a recycle delay time of 4 s and 80 accumulations. High power proton dipolar decoupling during the acquisition time was set at 80 kHz. The phosphorus chemical shift scale was calibrated to orthophosphoric acid (H_3PO_4) at 0 ppm. The ^{31}P CP/MAS NMR measurements were performed on the MPA, PPA, BPA, HPA, 4ABPA, and 6AHPA precursors used for surface grafting.

X-ray photoelectron spectroscopy (XPS) was performed on a Physical Electronics VersaProbe III Photoelectron Spectroscope with an Al Kα monochromatic X-ray source (1486.71 eV photon energy). The powders were applied on Scotch tape and the vacuum in the analysis chamber was approximately 7×10^{-7} Pa during measurements. Measurements were performed with a take-off angle of 45° with respect to the sample surface. High-resolution scans of the Ti 2p, O 1s, C 1s, P 2p, and N 1s photoelectron peaks were recorded from a spot diameter of 100 µm using a pass energy of 26 eV and a step size of 0.1 eV. The obtained data were analyzed with PHI Multipak and CasaXPS software. Prior to curve fitting, the energy scale of the XPS spectra was calibrated relative to the binding energy of Ti $2p_{3/2}$ (458.5 eV). [42]. Curve fitting was done after a Shirley-type background removal, using mixed Gaussian (80 - 100 %) - Lorentzian shapes. For the relative quantification of the different components in the N 1s spectra, the area of the fitted peaks was used. Two measurements were performed for each sample and the reported percentual contributions of the N 1s components have an experimental error of 3 %.

Zeta potential measurement on unmodified TiO_2 P25 was performed on a Zetasizer Nano ZS analyzer from Malvern Panalytical equipped with a He-Ne laser (633 nm). The measurement cell consisted of a folded capillary cell of polycarbonate with gold-coated electrodes. To maintain a constant ionic strength during the pH adjustment, the sample (75 mg) was dispersed in 50 mL of a 10 mM aqueous KCl solution. To adjust the pH, diluted solutions of HCl and NaOH with concentrations of 100, 10, and 1 mM were used. The temperature was maintained at a constant 25 °C during the measurement. The IEP was determined via interpolation.

2.3 Quantum chemical calculations

Density-functional theory (DFT) calculations were performed under Periodic Boundary Conditions (PBC) with the Quantum Espresso (QE) software package [43]–[45] using plane waves as basis sets. The Wu & Cohen (WC) modification of the Perdew-Burke-Ernzerhof (PBE) functional [46] was used since it allows for a high-quality description of solid-state materials [47]. Treatment of the core electrons was based on the projector augmented wave (PAW) method [48]. The $1s^2$ electrons were treated as core electrons for C, O, and N, whereas the $1s^2 2s^2 2p^6$ electrons were treated as core electrons for Ti and P. An energy cutoff of 60 Ry and a k-point grid of $2 \times 2 \times 1$ were used. Dispersion interactions were taken into account by adding a term to the DFT total energy based on the DFT-D2 method by Grimme [49], [50].

The anatase (101) facet was selected as the substrate since it is the most exposed facet (~ 94 %) in the anatase crystal phase [51], which is the most abundant phase in TiO_2 P25 [52], [53]. A 3-layer slab with a 20 Å vacuum width was constructed using the cif2cell software package [54]. The atoms in the lowest layer of the slab were constrained to their bulk positions, while all other atoms were allowed to relax. Adsorption energies, E_{ads}, were calculated as $E_{ads} = E_{adsorbate+surface} - (E_{adsorbate} + E_{surface})$ in which $E_{adsorbate+surface}$ is the energy of the adsorption complex, while $E_{adsorbate}$ and $E_{surface}$ are the energies of the isolated adsorbate molecule and the clean surface, respectively. Since, however, adsorption energies become less and less relevant when multiple species are adsorbed on the surface, we have

chosen to report relative energies among the different calculated structures, setting the binding modes that contain an NH_3^+ moiety at 0 kJ/mol for each PA. Consequently, some of the reported energies are positive. Calculations of the ^{31}P chemical shifts were performed using the gauge-including projector augmented wave (GIPAW) method [55], as implemented in the QE software package. The isotropic chemical shift δ_{iso} was defined as $\delta_{iso} = -(\sigma-\sigma_{ref})$, berlinite ($AlPO_4$) with $\delta_{iso}(^{31}P) = -25.6$ ppm [56] referenced to H_3PO_4 was selected as the reference of the isotropic shielding to define $\sigma_{ref,calc}(^{31}P)$ in order to compare experimental and calculated chemical shifts. The final binding modes were rendered using the Vesta program [57].

3. Results and discussion

3.1 The influence of concentration and pH on the modification degree

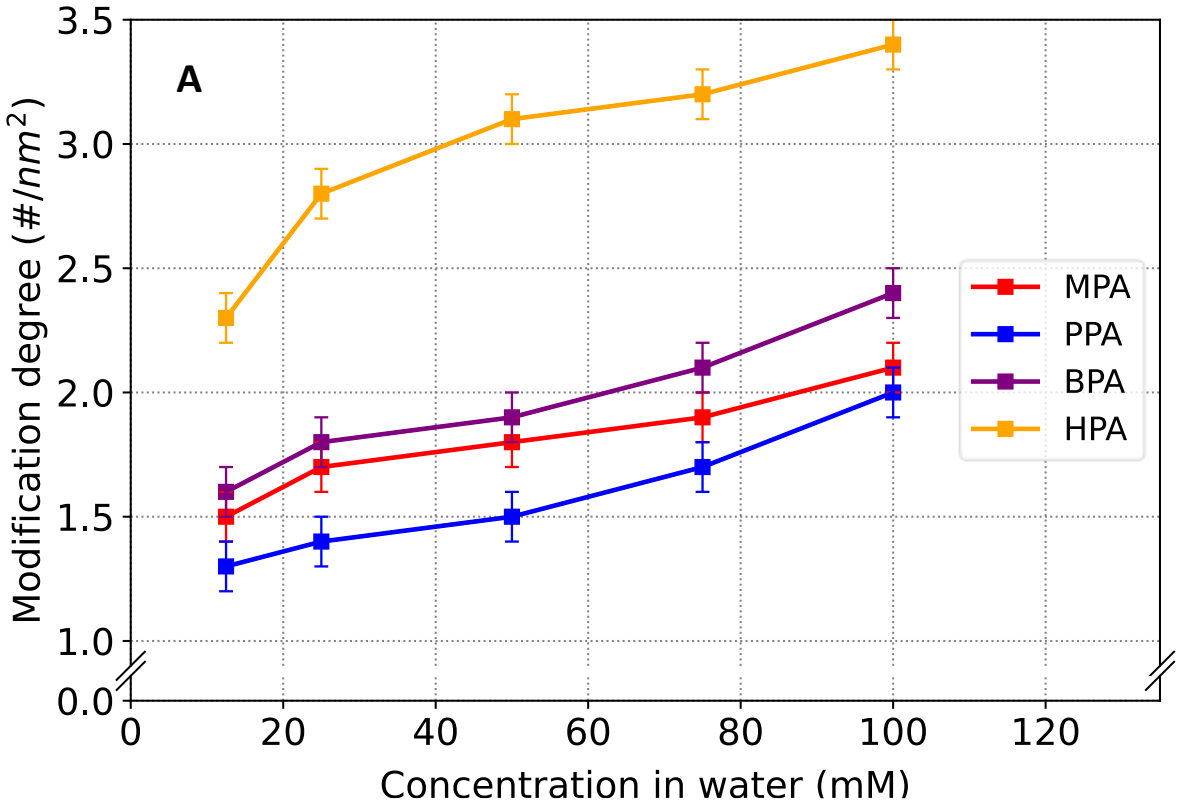

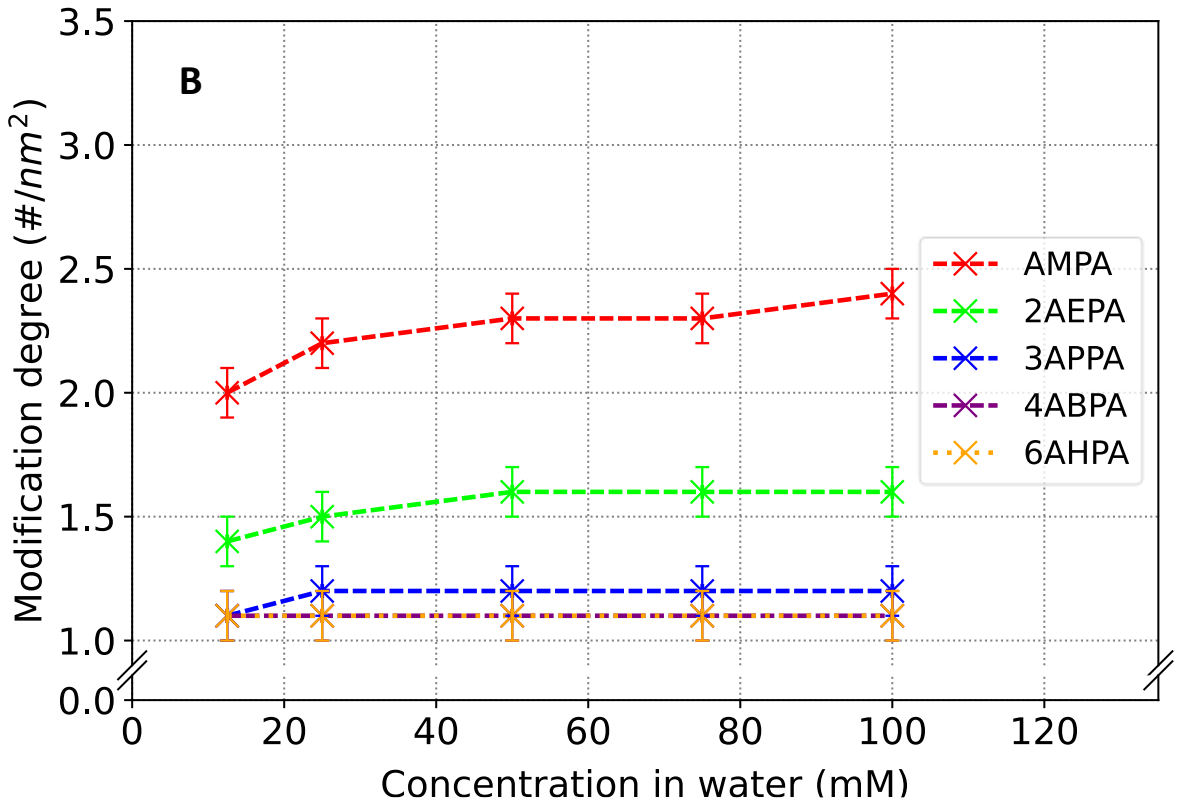

Figure 2. Influence of the PA solution concentration on modification degree for the TiO_2 P25 grafted with the alkylphosphonic acids (A) and the aminoalkylphosphonic acids (B). All samples were synthesized with a PA solution adjusted to pH 2. Note that the graphs of 4ABPA and 6AHPA are on top of each other.

The modification degrees of the TiO_2 P25 modified with 9 different organophosphonic acids (MPA, PPA, BPA, HPA, AMPA, 2AEPA, 3APPA, 4ABPA, and 6AHPA) at different concentrations are shown in Figure 2. The samples modified with alkylphosphonic acids (MPA, PPA, BPA, and HPA, Figure 2A) show an increasing modification degree with increasing PA concentration (MPA 1.5 - 2.1 groups/nm^2, PPA 1.3 - 2.0 groups/nm^2, BPA 1.6 - 2.4 groups/nm^2, HPA 2.3 - 3.4 groups/nm^2). Compared to MPA, PPA, and BPA samples, the HPA samples have the highest modification degrees. This could be related to a self-assembly effect due to the longer carbon chain, which has already been described in the literature [14], [58], [59].

However, since the calculation of the modification degree takes all phosphorous atoms into account (ICP-OES) or all organic chains burnt at elevated temperature (TGA), the previously mentioned titanium alkylphosphonate phase formation could also partly account for the calculated modification degrees. The formation of titanium alkylphosphonate layered structures is a possible side reaction during grafting, caused by a dissolution-precipitation process at the TiO_2 surface when synthesis is performed at elevated temperatures and high concentrations, inducing also a low pH. For the grafting of PPA on P25, a titanium propylphosphonate phase has previously been reported when grafting at a PPA concentration of 150 mM at 90 °C [19]. However, in the case of BPA, a titanium butylphosphonate phase can already form in the samples synthesized with a 100 mM solution at 90 °C. This is revealed by an additional ^{31}P NMR peak at 8 ppm in Figure 6 (discussed in section 3.2) and the extra weight loss in TGA between 400 and 500 °C in Figure 3. The weight losses between 220 - 400 °C are in the typical range for the carbon chain to be burnt off. Compared to the samples of 25mM, 50mM, and 75mM, there is an extra weight loss signal at 400 - 500 °C in the 100 mM sample, which might be assigned to titanium butylphosphonate, analogous to the samples modified with propylphosphonic acid, reported by Roevens et al. [19]. For HPA, a titanium hexylphosphonate phase was already formed with a 25 mM solution at 90 °C (Figure 7), which will be discussed in section 3.2. Hence, as the carbon chain length increases, the concentration at which the side reaction forming titanium alkylphosphonates starts to occur seems to decrease, thus at least partially contributing to the higher modification degree for BPA100mMpH2, HPA25mMpH2 and HPA100mMpH2 samples as the modification degrees increase with chain length (apart from MPA) and concentration.

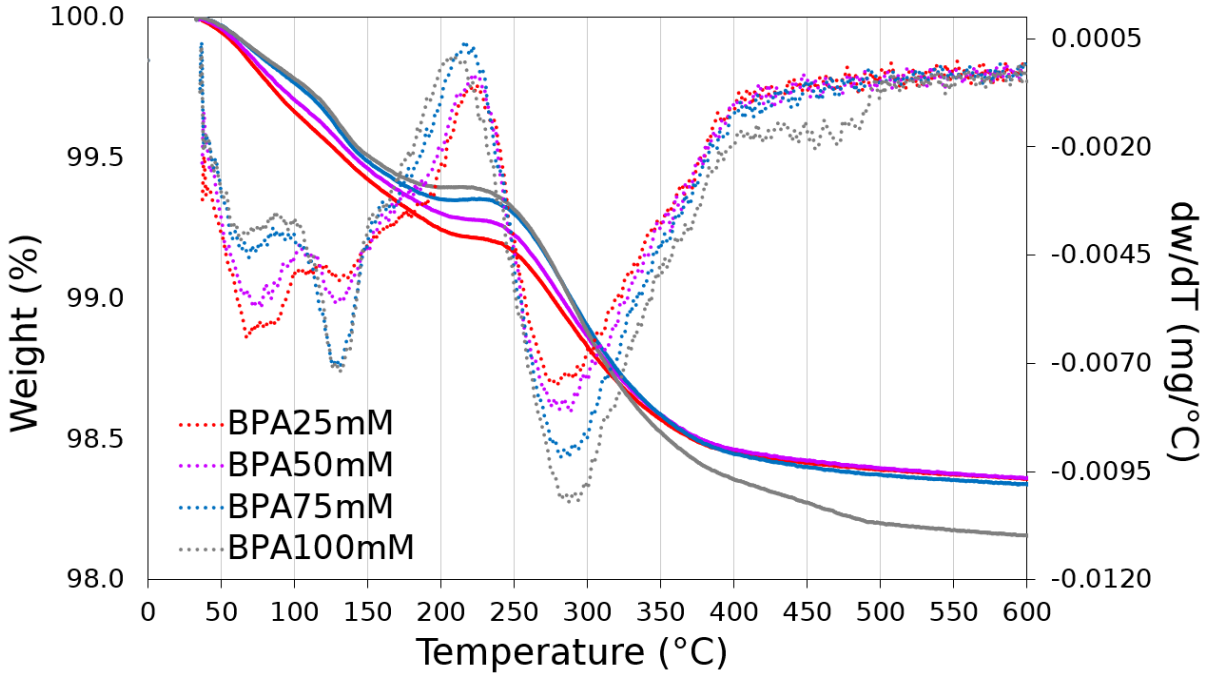

Figure 3. TGA/DTG patterns of BPA-modified samples synthesized with BPA solutions at pH 2 at 90 °C, the TGA measurements were performed under a constant oxygen flow of 80 mL/min.

When aminoalkylphosphonic acids were applied containing a terminal amine group, the samples showed a different trend (Figure 2B): the AMPA samples, with the shortest carbon chain, exhibit the highest modification degrees (2.0 - 2.4 groups/nm^2), followed by the 2AEPA samples (1.4 - 1.6 groups/nm^2). For a hydrocarbon chain length of 3 and above, the modification degree remains similar between 1.1 and 1.2 groups/nm^2 irrespective of the chain length (i.e. 3APPA, 4ABPA, and 6AHPA). Compared to the grafting of alkylphosphonic acids, a clear impact of the added amine functionality can thus be observed, which could be related to the previously reported additional interactions between the amine functionality and the TiO_2 surface (in that case TiO_2 Hombikat M311) [37]. Such interactions would result in the amino-alkyl chain bending back to the surface, disrupting the possible self-assembly process of the organic chains and shielding adjacent bonding sites for other phosphonic acids, leading to

lower modification degrees.

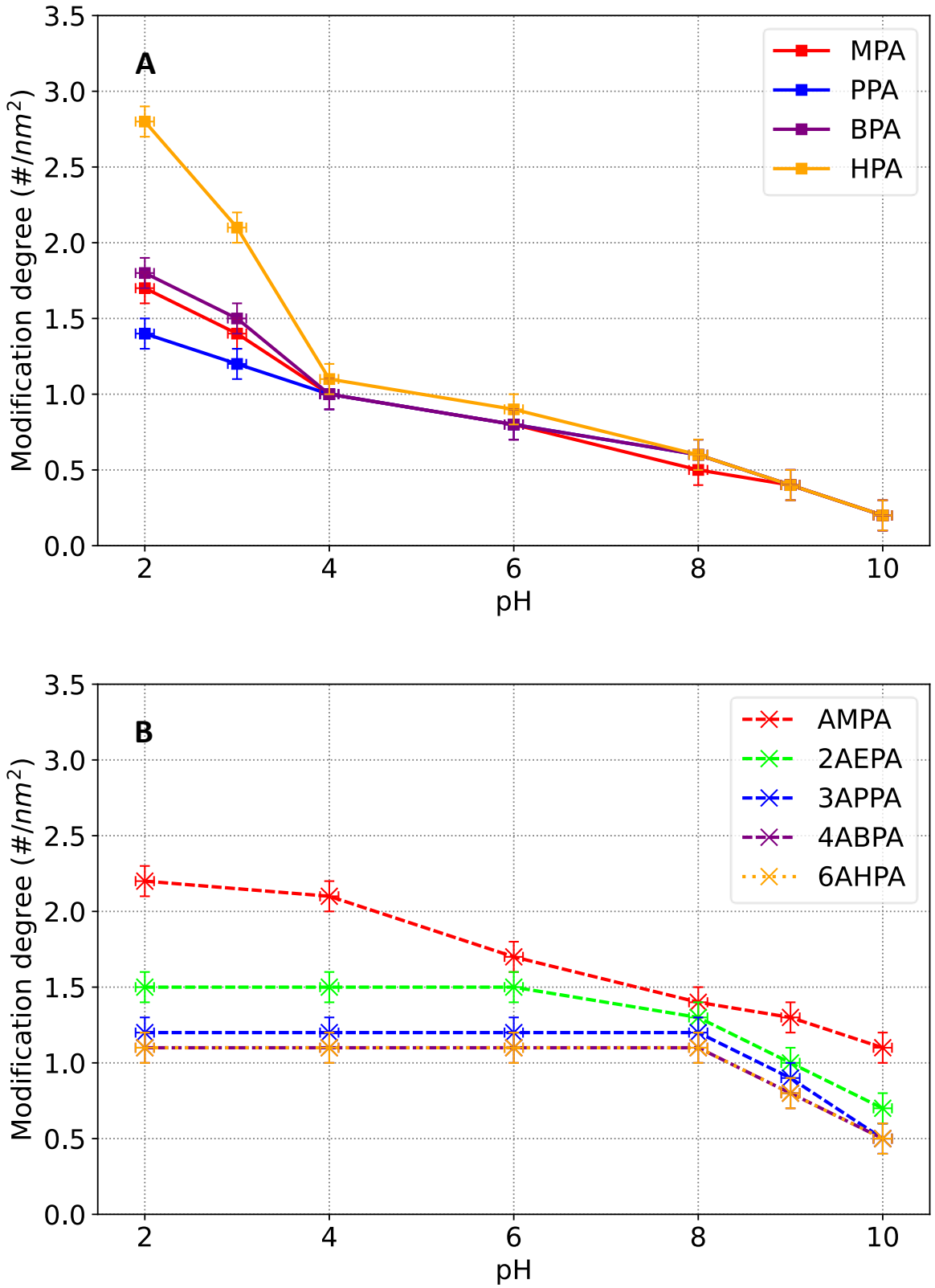

Figure 4. The influence of pH and hydrocarbon chain length on the modification degree for the TiO_2 P25 grafted with the alkylphosphonic acids (A) and the aminoalkylphosphonic acids

(B). All samples were synthesized with a concentration of 25 mM.

To study the effect of charges on the titania support during grafting with the alkylphosphonic acids and aminoalkylphosphonic acids, the pH of the PA solutions was adjusted before synthesis. The modification degrees of the resulting materials are shown in Figure 4. The modification degrees of the alkylphosphonic acids (MPA, PPA, BPA, and HPA, Figure 4A) decreased when the pH of the PA solutions was increased, with the most prominent decrease from pH 2 to pH 4. Subsequently, the modification degrees continue to decrease until pH 10. Moreover, between pH 4 and pH 10, little to no difference in the modification degrees can be observed for the different chain lengths in contrast to the clear differences in modification degrees below pH 4 (Figure 4A). However, the aminoalkylphosphonic acid grafted samples behaved differently (Figure 4B). Little to no change in modification degree was observed between pH 2 an pH 8 for grafted 3APPA, 4ABPA, and 6AHPA, followed by a decrease from pH 8 to pH 10. The 2AEPA samples showed a similar trend except that the decrease in modification degree already started from pH 6. In contrast, the modification degrees of the AMPA samples gradually decreased with increasing pH from 2 to 10, while they were the highest values with respect to the other aminoalkylphosphonic acids. Furthermore, at pH values above 4, the samples with an amine functionality exhibited higher modification degrees compared to their amine-free analogs.

The reported IEPs of anatase and rutile TiO_2 are around 5.3-6.0 [60]–[62], and the IEP of TiO_2 P25 was determined to be 6.6 by zeta potential measurement as shown in Figure 5. The surface of titania is negatively charged at pH values above the IEP due to surface $-O^-$ groups, whereas

below the IEP, the surface is positively charged due to the surface -OH_2^+ groups. Also, the charge and dissociation degree of the organophosphonic acids in an aqueous solution depends on the pH.

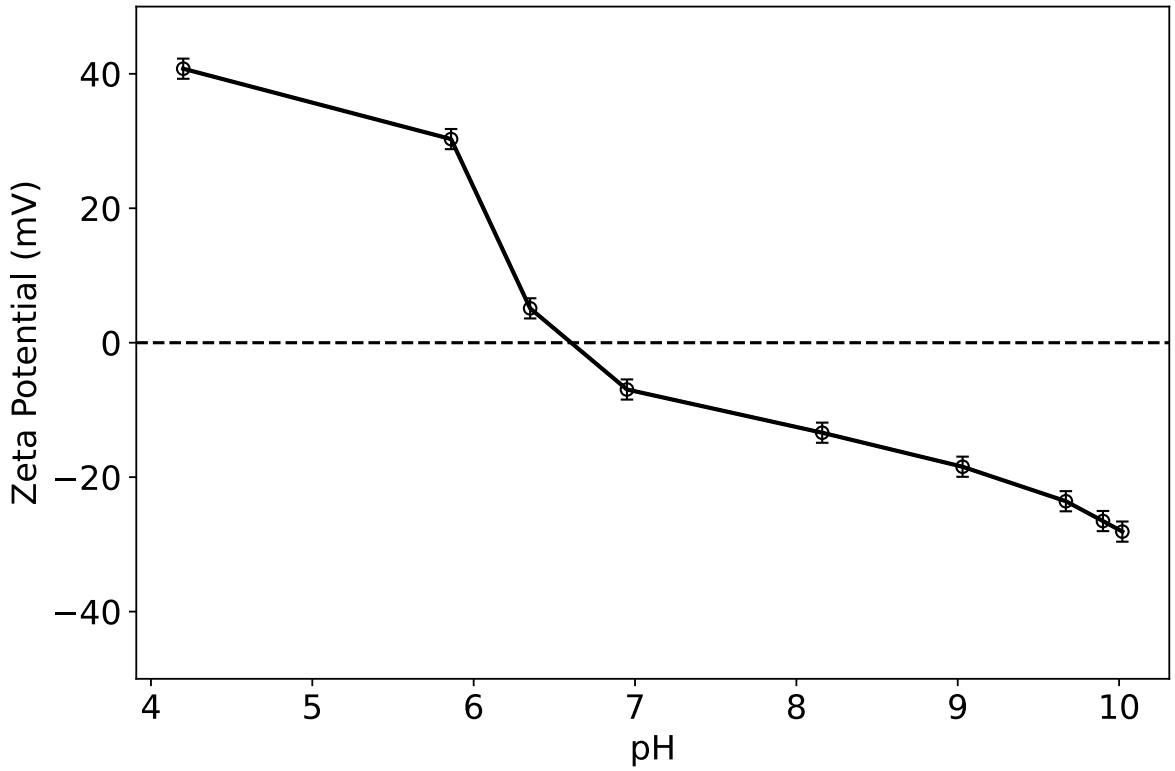

Figure 5. Zeta potential as a function of pH for TiO_2 P25. IEP determined to be 6.6.

The acid-base equilibria of the alkylphosphonic acids are:

$$R1\text{-}PO_3H_2\ (aq) + H_2O\ (l) \rightleftharpoons R1\text{-}PO_3H^-\ (aq) + H_3O^+\ (aq)\ (pK_{a1})$$

$$R1\text{-}PO_3H^-\ (aq) + H_2O\ (l) \rightleftharpoons R1\text{-}PO_3^{2-}\ (aq) + H_3O^+\ (aq)\ (pK_{a2})$$

With R1 = CH_3, $(CH_2)_2CH_3$, $(CH_2)_3CH_3$ or $(CH_2)_5CH_3$

In the case of aminoalkylphosphonic acids, the acid-base equilibria are:

$$NH_3^+\text{-}R2\text{-}PO_3H_2\ (aq) + H_2O\ (l) \rightleftharpoons NH_3^+\text{-}R2\text{-}PO_3H^-\ (aq) + H_3O^+\ (aq)\ (pK_{a1})$$

NH_3^+-R2-PO_3H^- (aq) + H_2O (l) ⇌ NH_3^+-R2-PO_3^{2-} (aq) + H_3O^+ (aq) (pK_{a2})

NH_3^+-R2-PO_3^{2-} (aq) + H_2O (l) ⇌ NH_2-R2-PO_3^{2-} (aq) + H_3O^+ (aq) (pK_{a3})

With R2 = CH_2, $(CH_2)_2$, $(CH_2)_3$, $(CH_2)_4$ or $(CH_2)_6$

Table 1. pK_a values of the PAs used in this work.

	pK_{a1}	**pK_{a2}**	**pK_{a3}**	**Ref**
MPA	2.38	7.74	-	[63]
PPA	2.49	8.18	-	[63]
BPA	2.59	8.19	-	[63]
HPA	2.6	7.9	-	[64]
AMPA	1.7	5.5	10.4	[38]
AMPA	1.8	5.4	10.0	[65]
AMPA	2.35	5.9	10.8	[66]
2AEPA	2.45	7.0	10.8	[66]
3APPA	2.0	7.0	11.4	[38]
3APPA	2.1	6.4	10.5	[67]
4ABPA	2.55	7.55	10.9	[66]
6AHPA	2.3	7.8	11.3	[38]

The literature reported pK_a values of the phosphonic acids used in this work are listed in Table 1. As the modification degrees of alkylphosphonic acid-modified samples decrease with increasing pH, it seems that the positive surface charge promotes the grafting process, although some influence of metal phosphonate formation cannot be excluded at pH 2 for grafting with BPA and HPA (as previously mentioned in section 3.1). The different behavior in function of the pH for the materials grafted with aminoalkylphosphonic acids shows again a critical impact

of the presence of the amine group. Between pK_{a1} and pK_{a3}, there is a combination of positive and negative charge(s) present (i.e. zwitterionic form) in the aminoalkylphosphonic acids in solution, resulting in both electrostatic attraction and repulsion with the surface, which could lead to more gradual changes in modification degrees in function of pH compared to the alkylphosphonic acids. In the pH range between 6 and 10, both the TiO_2 surface and the PAs are becoming more negatively charged, which could lead to electrostatic repulsion, causing the modification degrees to decrease. Nevertheless, the amine groups remain positively charged, which might promote the interactions between the amine-functionalized PAs and the surface, resulting in higher modification degrees than the alkylphosphonic acid-modified samples at pH > 4.

3.2 The chemical environment of phosphorus in the alkylphosphonic acid-modified materials at different pH values

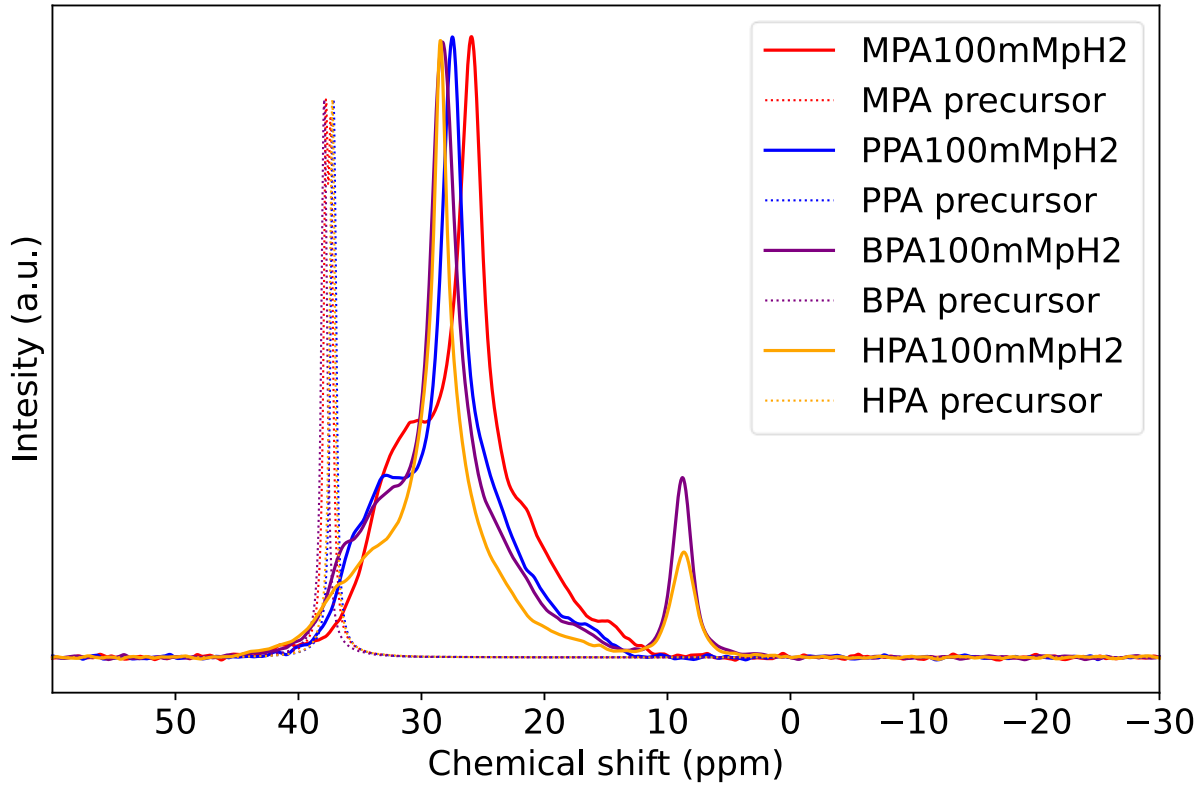

Figure 6. ^{31}P MAS NMR spectra of alkylphosphonic acid-modified samples (at pH = 2, solid lines) and ^{31}P CP/MAS NMR spectra of the PA precursors (dotted lines).

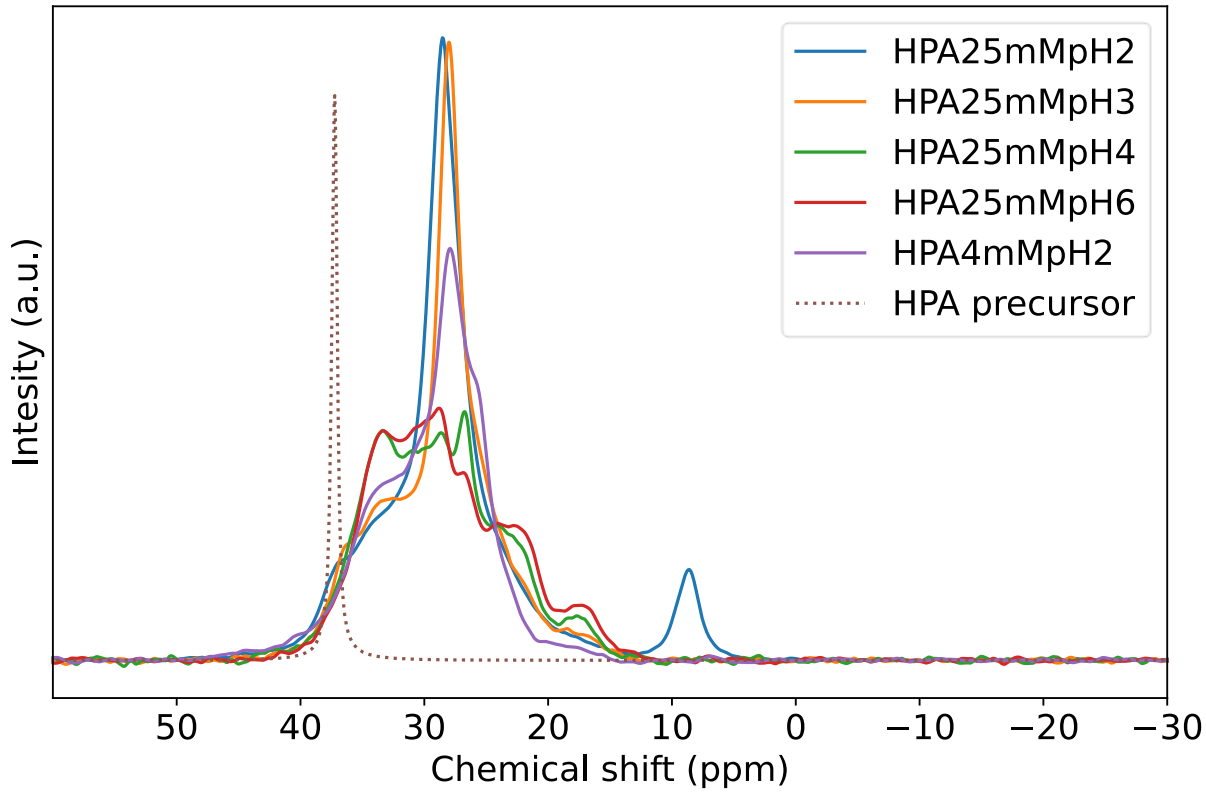

Figure 7. ^{31}P MAS NMR spectra of HPA-modified samples (at different pH values and concentrations) and ^{31}P CP/MAS NMR spectrum of the HPA precursor.

In order to correlate the differences in the modification degrees with differences in the phosphorus environments and the binding modes of the grafted PAs, as well as to gain more insight into the impact of the pH, the presence of the amine group and the hydrocarbon chain length on the chemical environment of phosphorus (especially the differences between AMPA, 2AEPA and the aminoalkylphosphonic acids with longer chains), ^{31}P CP/MAS NMR and ^{31}P MAS NMR measurements were performed on the precursors used for surface grafting and the modified materials in function of pH (Figures 6 - 9).

To confirm if the hydrocarbon chain length plays a role in the dissolution-precipitation reaction resulting in titanium phosphonate phases, the ^{31}P MAS NMR spectra of alkylphosphonic acid-modified samples with increasing chain length, prepared at pH 2, are shown in Figure 6. The main peak positions are located at 25.9 ppm, 27.5 ppm, 28.3 ppm, and 28.5 ppm for MPA, PPA, BPA, and HPA, respectively. The ^{31}P CP/MAS NMR spectra of the MPA, PPA, BPA, and HPA precursors are also shown in Figure 6, while more detailed spectra are shown in Figure S1. Hence, all grafted samples underwent an upfield shift compared to the alkylphosphonic acid precursors which display chemical shifts between 37 – 38 ppm. As the hydrocarbon chain length increased, an additional much more upfield peak with a chemical shift at 8 ppm appeared in the BPA and HPA samples. Such large upfield shifts have been observed before in PPA-modified and phenylphosphonic acid (PhPA)-modified samples [18], [19], and were assigned to the formation of titanium propylphosphonate and titanium phenylphosphonate phases, respectively. Hence, analogously, the 8 ppm signals in BPA and

HPA samples might be assigned to titanium butyl- and hexylphosphonate. Thus, the longer chain length (> 4 carbon atoms) seems to promote the formation of titanium alkylphosphonate under the applied synthesis conditions.

When elucidating the role of pH, it can be observed that the peak located at 8 ppm in both the BPA and HPA samples disappeared when the pH was increased to 3 (Figure S2 and Figure 7), suggesting that a pH below 3 is necessary to initiate the dissolution-precipitation processes. Since this is an undesired side reaction during modification, elevating the pH of PA solutions to 3 is effective to suppress this process. This also implies that the impact of pH on the modification degrees discussed in section 3.1 is not solely caused by titanium alkylphosphonate formation.

Above pH 3, multiple peaks appear between 40 and 15 ppm in the HPA-modified samples (Figure 7), rather than a main resonance signal with flanking shoulder peaks. This phenomenon can also be observed for the BPA, PPA, and MPA samples (Figures S2 - S4). To exclude the difference in modification degree as the underlying reason, an additional sample synthesized with a lower concentration but at pH 2 was measured (HPA4mMpH2 in Figure 7). This sample has a modification degree of 0.9 groups/nm^2, which is the same as the HPA25mMpH6 sample. In contrast to the pH6 sample, the NMR spectrum of the HPA4mMpH2 sample still reveals the main resonance signal at around 28 ppm, which indicates that the pH not only enables changes in the modification degree but also in the chemical environment of the phosphorus atom. A similar phenomenon was also observed in the MPA, PPA, and BPA samples (Figures S2 - S4).

The different ratios of the chemical environments of phosphorus might originate from the different binding modes of the PA molecules on the surface and/or different preferences of the PA molecules for different crystal facets and/or surface sites when the pH was altered and consequently also the charging behavior of the surface and PA molecules was changed.

3.3 The protonation degree of the amine functionality and the chemical environment of phosphorus in the aminoalkylphosphonic acids-modified materials as a function of pH

Table 2. Calculated NH_2/NH_3^+ ratio (±3 %) from XPS N1s spectra. The experimental error on the modification degree is estimated to be ±0.1 groups/nm^2 through repeated experiments.

Sample	Mod. Deg. (groups/nm^2)	NH_2/NH_3^+ ratio
AMPA150mMpH4	2.6	34/66
AMPA100mMpH2	2.5	38/62
AMPA25mMpH4	2.1	42/58
AMPA100mMpH6	2.0	43/57
AMPA6.3mMpH4	1.6	52/48
AMPA25mMpH8	1.4	55/45
AMPA25mMpH10	1.1	57/43
2AEPA100mMpH4	1.6	44/56
2AEPA25mMpH4	1.5	46/54
2AEPA25mMpH8	1.3	54/46
2AEPA25mMpH10	0.7	61/39
3APPA50mMpH4	1.2	64/36
3APPA100mMpH4	1.2	63/37
3APPA50mMpH8	1.2	63/37
3APPA50mMpH10	0.5	65/35
4ABPA25mMpH4	1.1	71/29
4ABPA100mMpH4	1.1	70/30

4ABPA25mMpH8	1.1	72/28
4ABPA25mMpH10	0.5	71/29
6AHPA50mMpH4	1.1	81/19
6AHPA100mMpH4	1.1	80/20
6AHPA50mMpH8	1.1	79/21
6AHPA50mMpH10	0.5	80/20

As discussed in the previous sections, the hydrocarbon chain length and pH value exhibit a clear impact on the surface modification with alkylphosphonic acids. For the aminoalkylphosphonic acids, the impact of the amine group in combination with the chain length and pH are evaluated in more detail in this section. XPS measurements on the samples modified with aminoalkylphosphonic acids provide information on the protonation degree of the amine groups. The N1s spectra consist of a broad asymmetric band that was fitted into two contributions corresponding to NH_2 (399.6 ± 0.1 eV) and NH_3^+ (401.4 ± 0.1 eV) groups [37], [68]. The ratios of NH_2/NH_3^+ peak area were calculated after peak fitting, and the results are shown in Table 2, while the corresponding XPS spectra can be found in Figure S5. It can be observed that the AMPA and 2AEPA samples possess a higher relative contribution of NH_3^+ compared to the samples with more than three carbon atoms in the aminoalkylphosphonic acids. For the AMPA and 2AEPA samples, the relative contribution of NH_3^+ increases with increasing modification degree (Figure S6), synthesized either with a different concentration or at a different solution pH. In contrast, it can be observed that neither the modification degree nor the pH has a significant influence on the relative percentage of NH_3^+ for the materials modified with 3APPA, 4ABPA, and 6AHPA. Furthermore, comparing materials modified with 3APPA,

4ABPA, and 6AHPA, the percentage of NH_3^+ groups decreases with increasing hydrocarbon chain length. Even though not in function of pH, a similar correlation between the modification degree, hydrocarbon chain length, and the NH_2/NH_3^+ ratio has also been observed for aminoalkylphosphonic acid grafted mesoporous TiO_2 Hombikat M311 with hydrocarbon chain lengths of 1, 3, and 6 [38].

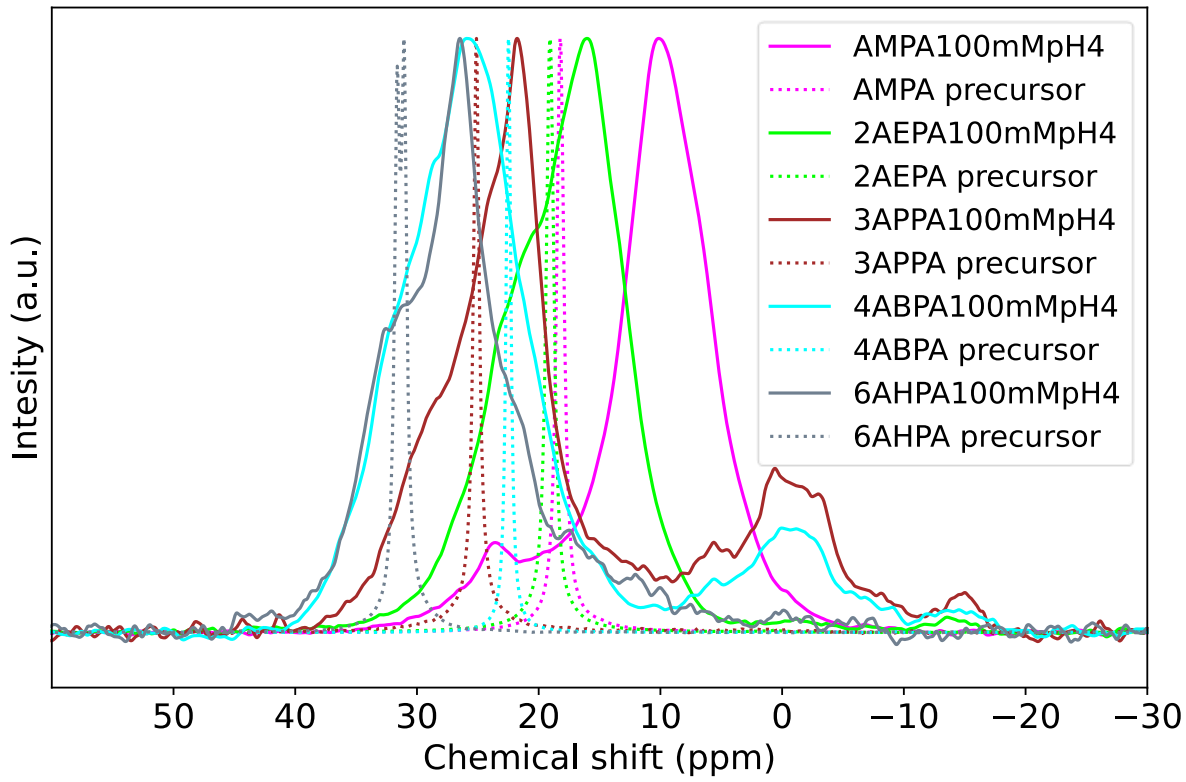

Figure 8. ^{31}P MAS NMR spectra of aminoalkylphosphonic acid-modified samples (at pH = 4, solid lines) and AMPA, 2AEPA, and 3APPA precursors (dotted lines), as well as ^{31}P CP/MAS NMR spectra of the 4ABPA and 6AHPA precursors (dotted lines). The ^{31}P NMR spectra are normalized by the intensities of their highest peaks.

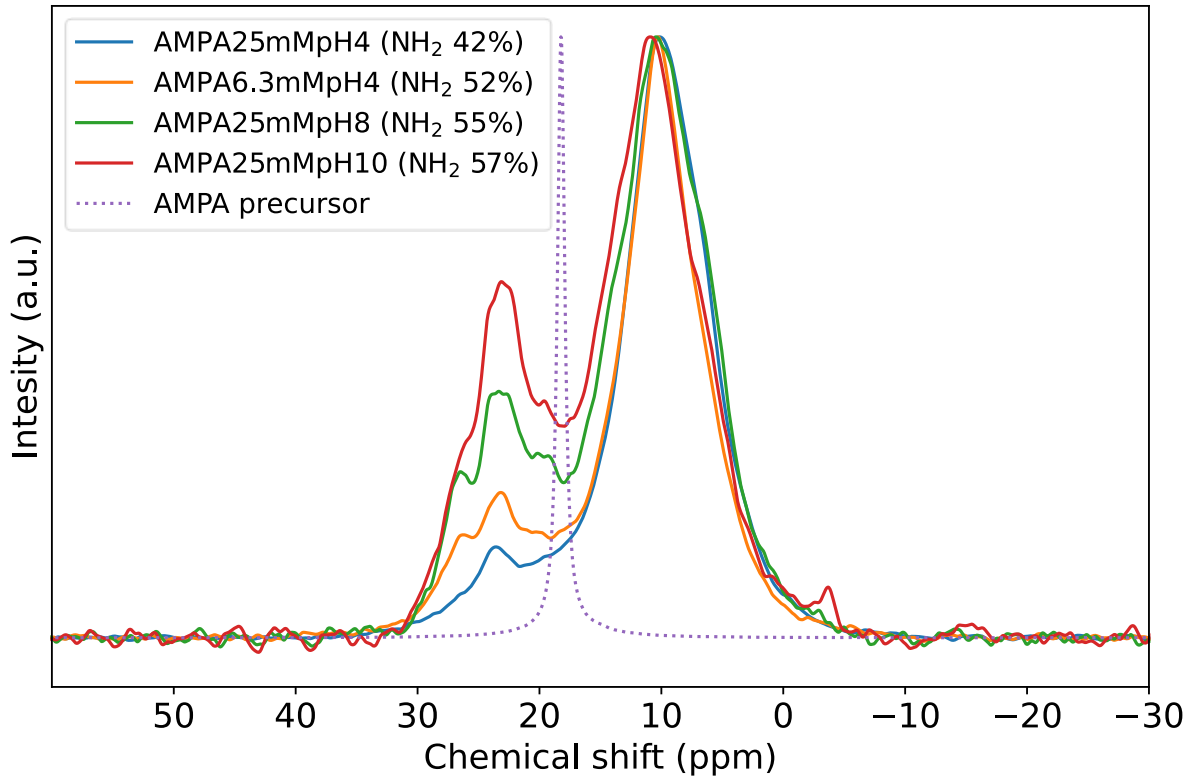

Figure 9. ^{31}P MAS NMR spectra of AMPA-modified samples (at different pH values and concentrations) with their NH_2 percentages obtained from XPS measurements listed in legend, as well as the ^{31}P MAS NMR spectrum of the AMPA precursor. The ^{31}P MAS NMR spectra are normalized by the intensities of their highest peaks to better illustrate the peak ratios, while the original intensities obtained from measurements are shown in Figure S7.

The influence of the amine functionality and the chain length on the chemical environment of phosphorus were studied by ^{31}P-NMR spectroscopy. The spectra of TiO_2 P25 samples modified with aminoalkylphosphonic acids at pH 4 as well as their precursors are shown in Figure 8. When evaluating the chemical shift of the main resonance signal, the 4ABPA grafted sample exhibits a downfield shift of 3.3 ppm with respect to the precursor resonance signal (from 22.6 ppm to 25.9 ppm), while all the other aminoalkylphosphonic acid-grafted samples exhibit upfield shifts. Furthermore, the AMPA grafted sample is characterized by a main resonance signal at around 10.2 ppm, revealing the largest shift (8.0 ppm) with respect to the precursor resonance signal at 18.2 ppm (Figure 8). The ^{31}P-NMR spectra of AMPA, 3APPA, and 6AHPA

grafted on a different type of TiO_2 (Hombikat 311) and without pH adjustment have been reported by Gys et al., and a relatively large upfield shift (9.0 ppm) of AMPA-grafted TiO_2 Hombikat 311 has also been observed [38]. In addition, the 3APPA and 4ABPA modified samples have several additional peaks in the region between -20 ppm and 10 ppm, which are subject for further investigation.

The impact of pH on the chemical environment of phosphorus has also been investigated. The ^{31}P-NMR spectra of the AMPA precursor and modified samples as a function of pH are shown in Figure 9 and Figure S7, and the spectra of the 2AEPA, 3APPA, 4ABPA, and 6AHPA samples are shown in Figures S8 – S11. Compared to the sharp resonance signal of the AMPA precursor at 18.2 ppm, all AMPA-modified P25 samples reveal an upfield shifted main resonance signal at around 10 - 11 ppm. Furthermore, there were also multiple, less intense, downfield shifted peaks in the range between 20 and 30 ppm. The relative intensities of the peaks above 20 ppm increased with an increasing relative percentage of NH_2 groups (Figure 9). This indicates that the main peak around 10 to 11 ppm may correlate with the NH_3^+ involved binding modes while the peaks between 20 and 30 ppm may be related to NH_2 involved binding modes. The ^{31}P-NMR spectra of 2AEPA-modified samples showed similar trends (Figure S8): the relative peak ratio of the peak around 16 ppm decreased compared to the peaks at 20 to 30 ppm as the NH_2 percentage increased. Since the amine groups in the aminoalkylphosphonic acids are protonated at the pH around the IEP of TiO_2 P25, the differences in the NH_2/NH_3^+ ratios might result from the interactions between the amine groups and the titania surface, which is further discussed in the DFT study.

For the 3APPA, 4ABPA, and 6AHPA modified samples, the relative peak intensities in the range of 10 – 40 ppm change when the chain length or the pH was varied. With increasing hydrocarbon chain length, the peak representing the most abundant phosphorus environment is found at a higher chemical shift, as shown in Figure 8. The ^{31}P NMR spectra of the 3APPA, 4ABPA, and 6AHPA modified samples (pH4, pH8 and pH10) are shown in Figures S9 – S11. Their pH10 samples all have a higher chemical shift for the most abundant phosphorus environment compared to the peak position in the spectra of the corresponding pH4 and pH8 samples, indicating changes in the relative number of different binding modes when the pH was changed. However, the impact of pH on these samples shows a distinct behavior compared to the alkylphosphonic acid-modified samples without the amine group (Figures 6 and 7, Figures S2 – S4), illustrating the impact of the added amine functionality.

The C values obtained from nitrogen and argon sorption using the Brunauer-Emmett-Teller (BET) theory [69] are shown in Figure 10. The C value obtained from the BET equation can be regarded as a measure of the interaction energy between the probing molecule and the solid surface [70]. Hence, for nitrogen sorption, this parameter can be used to monitor the increasing hydrophobicity of the surface when there are more PA molecules present on the surface [15], [20]. The C value would exhibit a decreasing trend when the hydrophobicity increases [20]. However, the C values obtained from nitrogen sorption (Figure 10A) of AMPA samples show an opposite trend compared to the samples modified with the other PAs. The C values obtained from nitrogen adsorption of the AMPA samples were higher than those of blank P25 (91) and

increased with increasing modification degree, in contrast to the other samples. This is probably due to the surface interaction with the quadrupole moment of the nitrogen atom and an increased surface polarity in AMPA with increasing modification degree, whereas the other samples show a decrease in polarity with increasing modification degree and have lower C values compared to blank P25. To validate the polarity as a cause of this divergent behavior, at least in part, the C values obtained from argon adsorption (Figure 10B) were plotted, as argon does not undergo specific interactions with the surface, in contrast to the quadrupolar interaction of nitrogen. As the AMPA samples have the same trend as the other PA-modified materials in argon sorption, it supports an enhanced surface interaction with the quadrupole moment of the nitrogen molecule, suggesting an increase in surface polarity with increasing modification degree and thus a unique interaction of the AMPA with the surface, as also visible in the divergent behavior of AMPA in ^{31}P-NMR and XPS. Apart from the AMPA samples, the C values obtained from nitrogen sorption for the 2AEPA samples are below the C value of unmodified P25 and decrease with increasing modification degree, but the C values are higher than the C values of the other PAs as well (Figure 10A), relating to the impact of the higher relative NH_3^+ contribution and the shorter hydrocarbon chain.

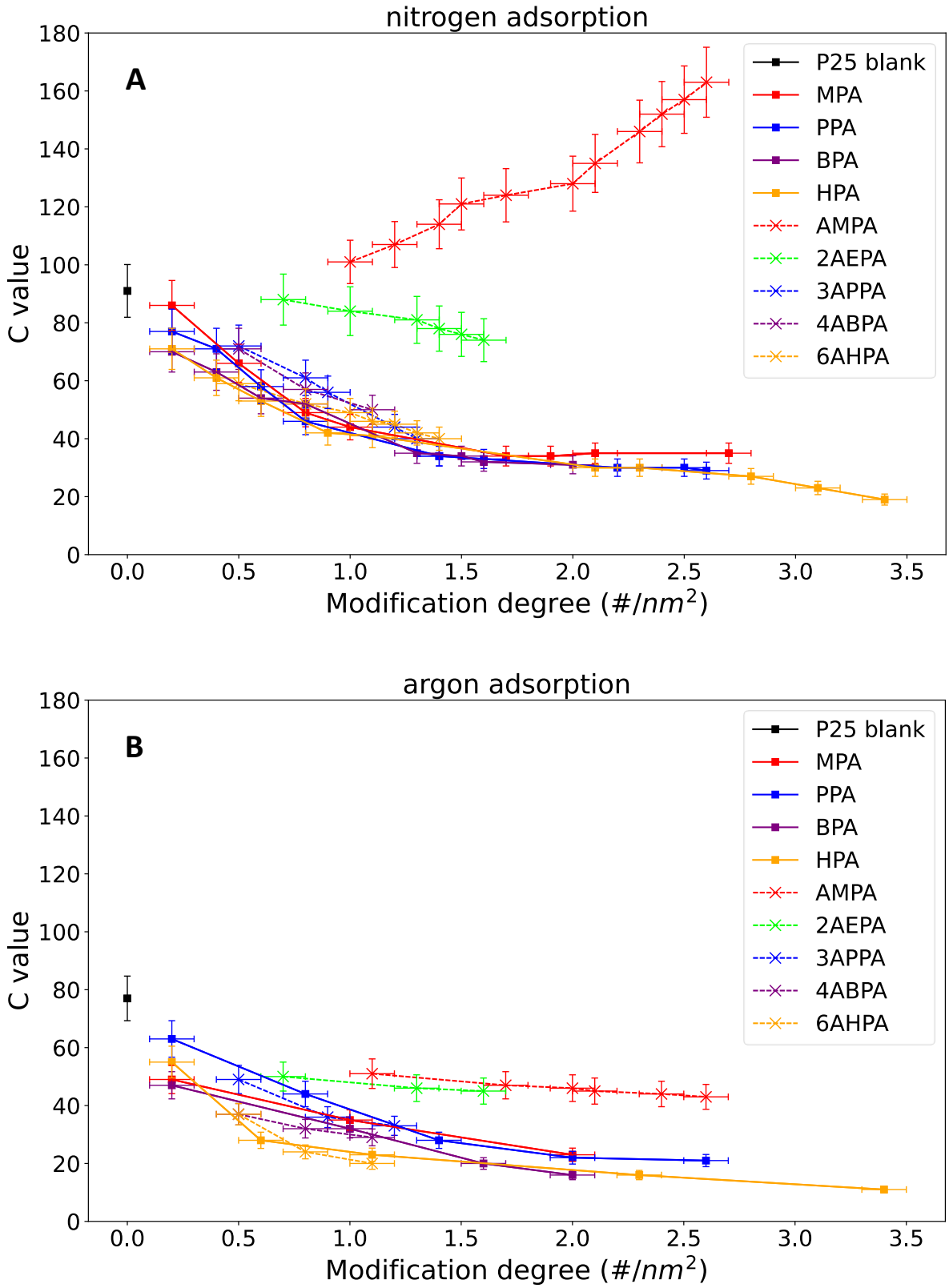

Figure 10. C values deduced from the BET equation as a function of modification degree. (A) nitrogen adsorption performed at -196°C, and (B) argon adsorption performed at -186°C.

In order to gain further insight into the link between these interactions, the NH_2/NH_3^+ ratio and their correlation with the phosphorus environments as a function of chain length, DFT calculations were performed. Since the dominant crystal surface of anatase is the (101) crystal facet and anatase accounts for about 83% of P25 [40], [71], [72], the DFT calculations were performed on PAs grafted on anatase (101) surfaces. Various binding modes with NH_2 or NH_3^+ were included in the models. The obtained binding modes of AMPA on the anatase (101) are shown in Figure 11, while their relative energies and ^{31}P-NMR chemical shifts are shown in Table 3. It is important to note that in order to illustrate the hydrogen bonding interactions, three AMPA molecules are shown in modes **5** and **6**, while in fact, there are only two molecules in the supercell used for the calculations (the molecules at the far right are identical to those on the far left). It is shown that the NH_3^+ groups can form short hydrogen bonds (H···O distances of 1.604 Å and 1.612 Å, mode **1**) with surface oxygen atoms, while the H···O distances of the hydrogen bonds formed between NH_2 and surface oxygen atoms are 2.404 Å and 2.405 Å, which are considerably longer (mode **3**); this fact may be used to explain the higher relative energy (46.3 kJ/mol) of the latter mode. On the other hand, the nitrogen atom in the NH_2 groups can also coordinate to surface Ti sites using its lone pair to form a Lewis acid-base interaction (Ti···NH_2). Yet, for AMPA grafted to TiO_2 (101), mode **1** (with an NH_3^+ functionality) has a lower energy than mode **2** (with a coordinating NH_2 group), and the difference is 22.5 kJ/mol. This stabilization can, however, become even greater when the NH_3^+ group interacts not only with a surface oxygen atom but also with a neighboring oxygen atom of the phosphonic acid group of an adjacent AMPA molecule: mode **4** is 31.0 kJ/mol per molecule more stable than

mode **1**. Interacting with a neighboring AMPA molecule also lowers the energies for modes **5** and **6**, which both contain (an) NH_2 group(s), although the per-molecule energy differences are much smaller than those reported above (11.3 and 2.2 kJ/mol for modes **5** and **6**, respectively, with respect to modes **2** and **3**, respectively).

This provides insights into the positive correlation between the NH_3^+ percentage and the modification degree from the XPS results of the AMPA samples. Although the calculated ^{31}P-NMR shifts of modes **1** and **4** are lower than the experimental value, chemical shifts around 9.6 - 10.7 ppm (Figure S12) were obtained when water molecules were added to mode **4** (modes **15** and **16** to which 4 and 8 water molecules were added, respectively), which are close to those of the main peaks in the ^{31}P-NMR spectra (Figure 9).

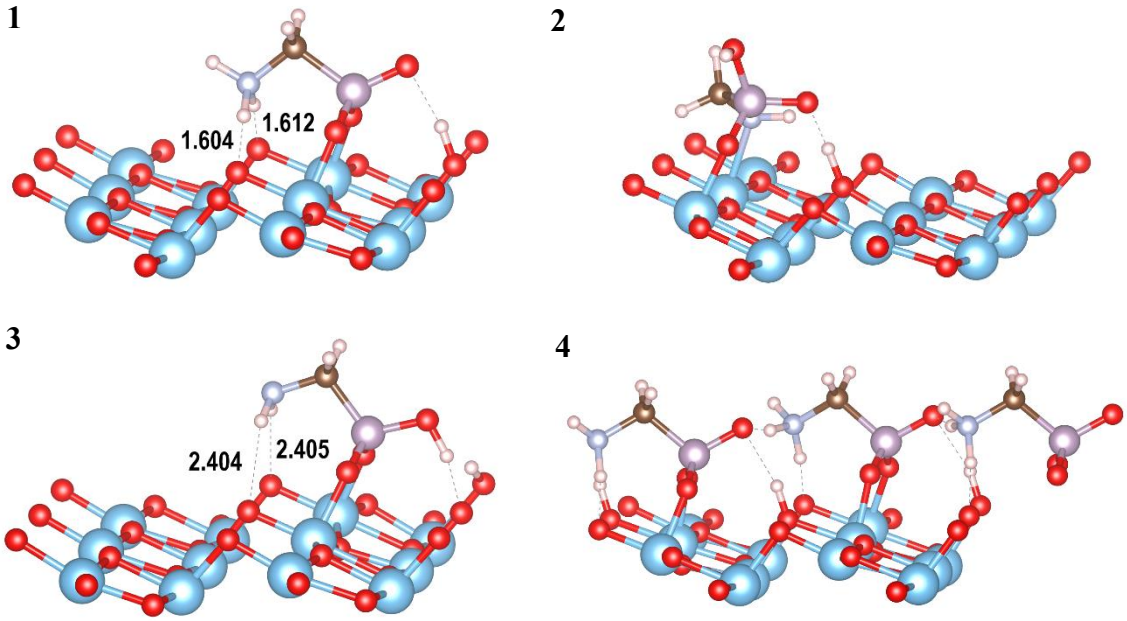

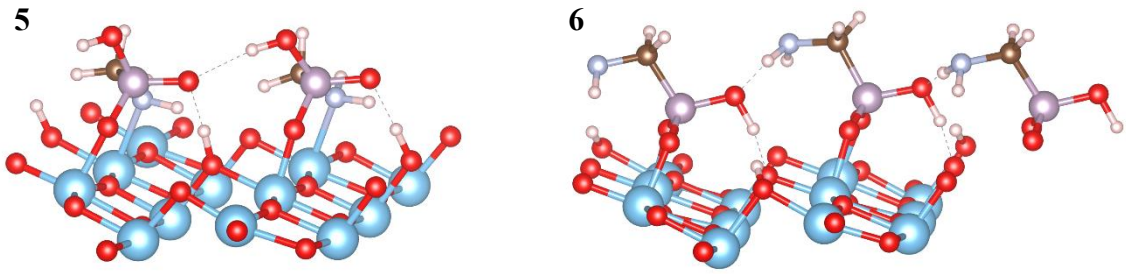

*Figure 11. Binding modes of AMPA on anatase (101) obtained from DFT calculations. The H···O distances (in Å) in modes **1** and **3** are indicated. Red, sky blue, purple, brown, cloudy blue and white spheres represent oxygen, titanium, phosphorous, carbon, nitrogen, and hydrogen atoms, respectively. Modes **1**, **2**, and **3** are with one AMPA molecule in the cell where **1** is with NH_3^+, while **2** and **3** are with NH_2. Modes **4**, **5**, and **6** are with two AMPA molecules in the supercell where **4** is with NH_3^+, while **5** and **6** are with NH_2.*

Table 3. Calculated relative energies and ^{31}P-NMR chemical shifts of the AMPA binding modes listed in Figure 11 (O_{AMPA} represents the oxygen atoms in AMPA, O_b represents the anatase (101) surface bridging oxygen atoms).

Binding mode	Number of AMPA molecules in supercell	TiO_2-PA interaction	Chemical state of the amine group	AMPA-surface and AMPA-AMPA interactions	Relative energies (kJ/mol)	$\delta(^{31}P)$ (ppm)
1	1	bidentate	NH_3^+	N-H···O_b interactions	0	-2.5
2	1	monodentate	NH_2	Ti···NH_2 interaction	+22.5	19.2
3	1	bidentate	NH_2	N-H···O_b interactions	+46.3	22.8
4	2	bidentate	NH_3^+	N-H···O_b interaction, intermolecular N-H···O_{AMPA} interaction	-31.0 (per molecule)	3.5, 3.4
5	2	monodentate	NH_2	Ti···NH_2 interaction, intermolecular O_{AMPA}-H···O_{AMPA} interaction	+11.2 (per molecule)	15.8, 11.9
6	2	bidentate	NH_2	N-H···O_b interaction, intermolecular	+44.1 (per molecule)	24.4, 24.4

				N-H···O_{AMPA} interaction		

The obtained lowest-energy binding modes for 2AEPA, 3APPA, 4ABPA, and 6AHPA with NH_2 or NH_3^+ on the anatase (101) are shown in Figure 12, while their relative energies and ^{31}P-NMR chemical shifts are shown in Table 4. The DFT calculations for 2AEPA grafted on the anatase (101) show the same trend as AMPA (mode **7** with an NH_3^+ group have lower adsorption energy), while the calculations for 3APPA, 4ABPA, and 6AHPA grafted on the anatase (101) exhibit an opposite trend: modes **10**, **12**, and **14** with an interaction between an NH_2 group and a surface Ti site are more energetically favorable. This difference may relate to the fact that AMPA and 2AEPA molecules grafted on the anatase (101) have to sacrifice one of the hydrogen bonds between a P-OH and a surface oxygen atom in order to form the bond between NH_2 and the surface, hampering the formation of a bidentate binding mode that creates extra stabilization (see mode **2** in Figure 11 and mode **8** in Figure 12). 2AEPA-NH_3^+ (mode **7**) is still more stable than that 2AEPA-NH_2 (mode **8**) by 19.0 kJ/mol. The associated calculated ^{31}P-NMR shifts are 16.2 and 24.1 ppm, respectively (Table 4), which coincide with the maxima of the most abundant peaks in the NMR spectra of the pH4/pH8 samples and pH10 samples, respectively (Figure S8).

Upon extension of the carbon chain length, the NH_2 binding mode becomes more energetically favorable. For 3APPA (modes **9** and **10**), 4ABPA (modes **11** and **12**) and 6AHPA (modes **13** and **14**) the differences are 0.9, 14.0 and 18.4 kJ/mol, each time in favor of the amine binding mode. It is interesting to note that the relative stabilization of the latter increases with increasing

carbon chain length and this is completely in line with the results of the XPS measurements given in Table 2.

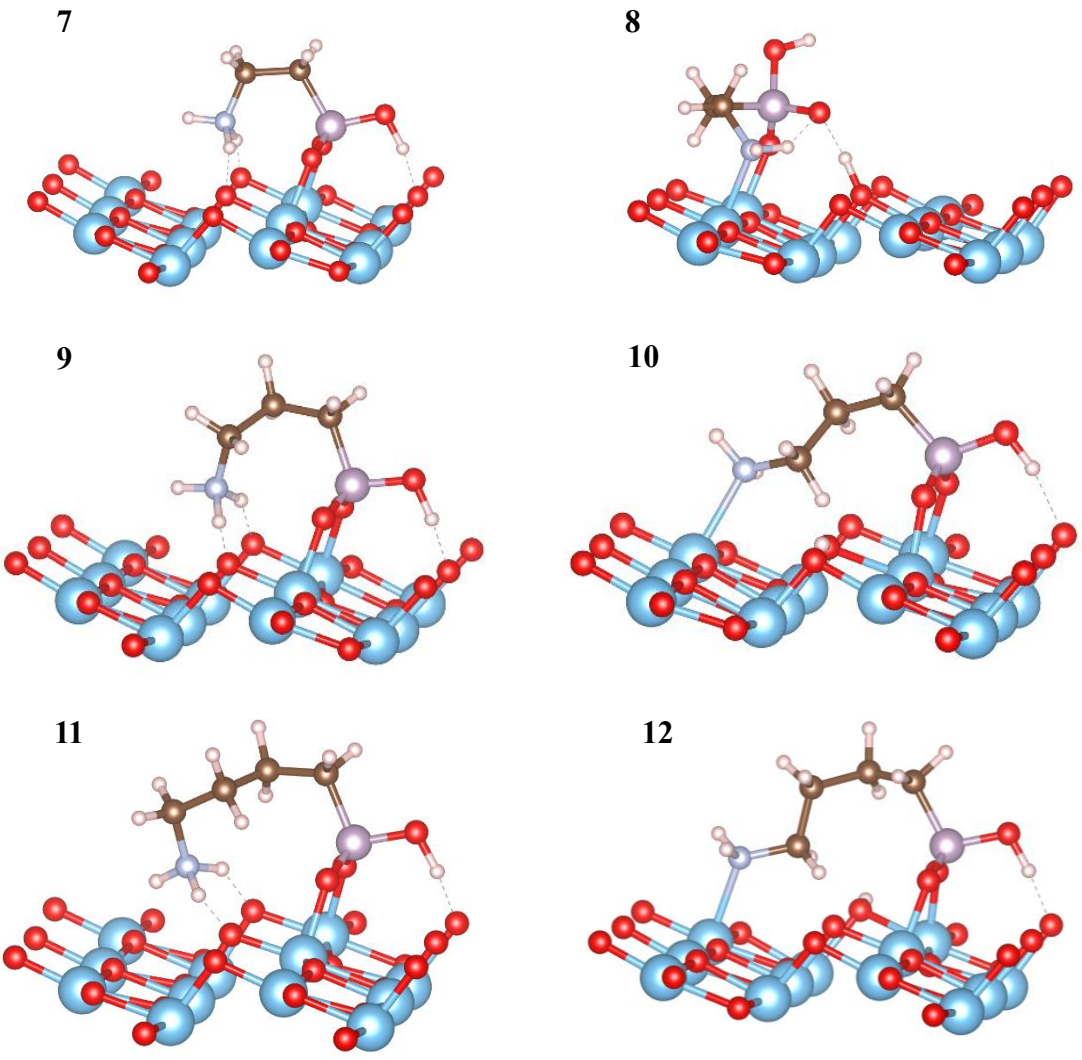

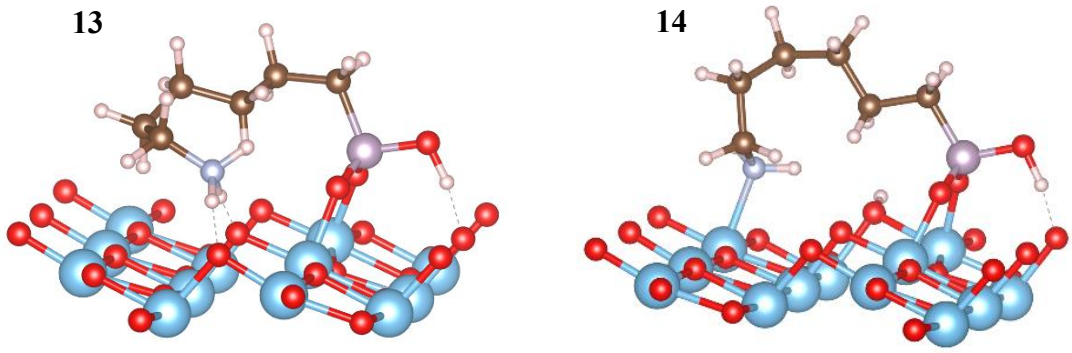

*Figure 12. Binding modes of 2AEPA (**7** and **8**), 3APPA (**9** and **10**), 4ABPA (**11** and **12**), and 6AHPA (**13** and **14**) on anatase (101) obtained from DFT calculations. Red, sky blue, purple, brown, cloudy blue and white spheres represent oxygen, titanium, phosphorous, carbon, nitrogen, and hydrogen atoms, respectively.*

Table 4. Calculated relative energies for each of the adsorbates and ^{31}P-NMR chemical shifts of the binding modes listed in Figure 12 (O_b represents the anatase (101) surface bridging oxygen atoms).

PA molecule	Binding mode	TiO_2-PA interaction	Chemical state of the amine group	Adsorbate-surface interaction	Relative energies (kJ/mol)	$\delta(^{31}P)$ (ppm)
2AEPA	**7**	bidentate	NH_3^+	N-H···O_b interactions	0	16.2
	8	monodentate	NH_2	Ti···NH_2 interaction	+19.0	24.1
3APPA	**9**	bidentate	NH_3^+	N-H···O_b interactions	0	22.4
	10	bidentate	NH_2	Ti···NH_2 interaction	-0.9	28.5
4ABPA	**11**	bidentate	NH_3^+	N-H···O_b interactions	0	25.9
	12	bidentate	NH_2	Ti···NH_2 interaction	-14.0	29.0
6AHPA	**13**	bidentate	NH_3^+	N-H···O_b interactions	0	26.8
	14	bidentate	NH_2	Ti···NH_2 interaction	-18.4	28.4

4. Conclusions

TiO_2 P25 was modified with alkylphosphonic acids and aminoalkylphosphonic acids with varying hydrocarbon lengths (C1 to C6). Samples were synthesized at different concentrations and with the pH of the PA solutions adjusted to different values between 2 and 10.

From the results, it can be concluded that:

(1) The surface modification degrees of the alkylphosphonic acids and AMPA were in general decreasing when the pH increased in contrast to 2AEPA, 3APPA, 4ABPA, and 6AHPA, which have almost constant modification degrees between pH 2 and 8 (6 for 2AEPA), proving a clear impact of the presence of the amine group.

(2) Increasing the pH to 3 or higher was proven to eliminate the dissolution-precipitation side reaction, preventing the undesired formation of titanium alkylphosphonates.

(3) Furthermore, ^{31}P-NMR revealed a significant impact of pH on the phosphorus chemical environment of the alkylphosphonic acid grafted on TiO_2.

(4) XPS N1s and ^{31}P-NMR showed that the AMPA- and 2AEPA- modified samples have higher NH_3^+ to NH_2 ratios compared to the PAs with longer carbon chains. This was confirmed by the results of DFT calculations that explain why binding modes in which the NH_3^+ groups are interacting with the surface oxygen atoms are more energetically favorable for AMPA and 2AEPA, while the opposite is true for the aminoalkylphosphonic acids with carbon chains of three or more carbon atoms.

(5) Moreover, the calculations provided insight into the AMPA-AMPA interactions at the surface that might explain the divergent increasing surface polarity with increasing

surface modification degrees.

This work provides insights into the correlation between the organic chain length and the nature of the species at the surface. Moreover, it provides insights into the ability to alter surface properties by adjusting concentration and pH during surface modification. With this knowledge, the surface properties can be adapted for specific applications by varying the carbon chain length, adding the amine functionality, and customizing the synthesis conditions (e.g. concentration or pH).

Funding sources

R. An is grateful for the support of the DOCPRO4 project of the University of Antwerp. N. Gys was supported by a VITO PhD scholarship. The Research Foundation Flanders (FWO Vlaanderen) and Hasselt University are acknowledged for the financial support of this research via the Hercules project AUHL/15/2-GOH3816N. The DFT calculations were performed using the Leibnitz HPC infrastructure at the CalcUA core facility of the University of Antwerp, a division of the Flemish Supercomputer Center (VSC), funded by the Hercules Foundation, the Flemish Government and the University of Antwerp. P. Adriaensens acknowledges the support of FWO project G.0121.17N and V. Meynen acknowledges the support of FWO project K801621N and BOF sabbatical funding of UAntwerp. The XPS VPIII was funded by FWO medium-scale infrastructure project I006220N.

Acknowledgments

The authors would like to gratefully acknowledge K. Leyssens, S. Defossé, W. Xu, and J. Wang for the nitrogen/argon sorption measurements (UAntwerp); K. Duyssens, F. Beutels and W. Brusten for the ICP-OES measurements (VITO); K. Leyssens, S. Defossé, B. M. Ramesha, and K. Zhang for the TGA measurements (UAntwerp); A. Vansant and H. Lenaerts for the zeta potential measurement (VITO).

CRediT authorship contribution statement

Rui An: Conceptualization, Investigation, Methodology, Visualization, Writing - original draft. **Lourdes Chukiwanka Quiñones:** Investigation, Methodology, Validation, Visualization. **Nick Gys:** Methodology, Writing - review & editing, Visualization. **Elien Derveaux:** Investigation, Methodology, Validation, Visualization. **Kitty Baert:** Investigation, Methodology, Validation, Visualization. **Tom Hauffman:** Methodology, Supervision, Writing - review & editing. **Peter Adriaensens:** Methodology, Supervision, Writing - review & editing. **Frank Blockhuys:** Supervision, Methodology, Investigation, Validation, Visualization, Writing - review & editing. **Vera Meynen:** Supervision, Conceptualization, Methodology, Validation, Writing - review & editing.

References

[1] V. Meynen, H. Castricum, and A. Buekenhoudt, “Class II Hybrid Organic-inorganic Membranes Creating New Versatility in Separations,” *Curr. Org. Chem.*, vol. 18, no. 18, pp. 2334–2350, 2014, doi: 10.2174/13852728196661408062009 31.

[2] S. Hosseinabadi, K. Wyns, A. Buekenhoudt, B. Van Der Bruggen, and D. Ormerod,

"Performance of Grignard functionalized ceramic nanofiltration membranes," *Sep. Purif. Technol.*, vol. 147, pp. 320–328, 2015, doi: 10.1016/j.seppur.2015.03.047.

[3] G. Mustafa, K. Wyns, P. Vandezande, A. Buekenhoudt, and V. Meynen, "Novel grafting method efficiently decreases irreversible fouling of ceramic nanofiltration membranes," vol. 470, pp. 369–377, 2014, doi: 10.1016/j.memsci.2014.07.050.

[4] G. Mustafa, K. Wyns, A. Buekenhoudt, and V. Meynen, "New insights into the fouling mechanism of dissolved organic matter applying nanofiltration membranes with a variety of surface chemistries," *Water Res.*, vol. 93, pp. 195–204, 2016, doi: 10.1016/j.watres.2016.02.030.

[5] C. R. Silva, C. Airoldi, K. E. Collins, and C. H. Collins, "Influence of the TiO_2 content on the chromatographic performance and high pH stability of C18 titanized phases," *J. Chromatogr. A*, vol. 1114, no. 1, pp. 45–52, 2006, doi: 10.1016/j.chroma.2006.02.025.

[6] C. W. Hsu, L. Wang, and W. F. Su, "Effect of chemical structure of interface modifier of TiO_2 on photovoltaic properties of poly(3-hexylthiophene)/TiO_2 layered solar cells," *J. Colloid Interface Sci.*, vol. 329, no. 1, pp. 182–187, 2009, doi: 10.1016/j.jcis.2008.10.008.

[7] S. W. Chong, C. W. Lai, J. C. Juan, and B. F. Leo, "An investigation on surface modified TiO_2 incorporated with graphene oxide for dye-sensitized solar cell," *Sol. Energy*, vol. 191, no. July, pp. 663–671, 2019, doi: 10.1016/j.solener.2019.08.065.

[8] C. Wang, L. Yin, L. Zhang, D. Xiang, and R. Gao, "Metal oxide gas sensors: Sensitivity and influencing factors," *Sensors*, vol. 10, no. 3, pp. 2088–2106, 2010, doi: 10.3390/s100302088.

[9] A. Mitrofanov, S. Brandès, F. Herbst, S. Rigolet, A. Bessmertnykh-Lemeune, and I. Beletskaya, "Immobilization of copper complexes with (1,10-phenanthrolinyl)phosphonates on titania supports for sustainable catalysis," *J. Mater. Chem. A*, vol. 5, no. 24, pp. 12216–12235, 2017, doi: 10.1039/c7ta01195d.

[10] H. Tada, Q. Jin, A. Iwaszuk, and M. Nolan, "Molecular-scale transition metal oxide nanocluster surface-modified titanium dioxide as solar-activated environmental catalysts," *J. Phys. Chem. C*, vol. 118, no. 23, pp. 12077–12086, 2014, doi:

10.1021/jp412312m.

[11] N. Adden, L. J. Gamble, D. G. Castner, A. Hoffmann, G. Gross, and H. Menzel, "Phosphonic acid monolayers for binding of bioactive molecules to titanium surfaces," *Langmuir*, vol. 22, no. 19, pp. 8197–8204, 2006, doi: 10.1021/la060754c.

[12] H. Sharma, K. Kumar, C. Choudhary, P. K. Mishra, and B. Vaidya, "Development and characterization of metal oxide nanoparticles for the delivery of anticancer drug," *Artif. Cells, Nanomedicine Biotechnol.*, vol. 44, no. 2, pp. 672–679, 2016, doi: 10.3109/21691401.2014.978980.

[13] J. Randon, P. Blanc, and R. Paterson, "Modification of ceramic membrane surfaces using phosphoric acid and alkyl phosphonic acids and its effects on ultrafiltration of BSA protein," *J. Memb. Sci.*, vol. 98, no. 1–2, pp. 119–129, 1995, doi: 10.1016/0376-7388(94)00183-Y.

[14] W. Gao, L. Dickinson, C. Grozinger, F. G. Morin, and L. Reven, "Self-Assembled Monolayers of Alkylphosphonic Acids on Metal Oxides," *Langmuir*, vol. 12, no. 26, pp. 6429–6435, 1996, doi: 10.1021/la9607621.

[15] G. Guerrero, P. H. Mutin, and A. Vioux, "Anchoring of Phosphonate and Phosphinate Coupling Molecules on Titania Particles," *Chem. Mater.*, no. 13, pp. 4367–4373, 2001, doi: 10.1039/B104411G.

[16] P. H. Mutin, V. Lafond, A. F. Popa, M. Granier, L. Markey, and A. Dereux, "Selective surface modification of SiO_2-TiO_2 supports with phosphonic acids," *Chemistry of Materials*, vol. 16, no. 26. pp. 5670–5675, 2004, doi: 10.1021/cm035367s.

[17] S. Tosatti, R. Michel, M. Textor, and N. D. Spencer, "Self-assembled monolayers of dodecyl and hydroxy-dodecyl phosphates on both smooth and rough titanium and titanium oxide surfaces," *Langmuir*, vol. 18, no. 9, pp. 3537–3548, 2002, doi: 10.1021/la011459p.

[18] M. Tassi *et al.*, "A detailed investigation of the microwave assisted phenylphosphonic acid modification of P25 TiO_2," *Adv. Powder Technol.*, vol. 28, no. 1, pp. 236–243, 2017, doi: 10.1016/j.apt.2016.09.020.

[19] A. Roevens *et al.*, "Revealing the influence of the solvent in combination with

temperature, concentration and pH on the modification of TiO_2 with 3PA," *Mater. Chem. Phys.*, vol. 184, pp. 324–334, 2016, doi: 10.1016/j.matchemphys.2016.09.059.

[20] A. Roevens *et al.*, "Aqueous or solvent based surface modification: The influence of the combination solvent – organic functional group on the surface characteristics of titanium dioxide grafted with organophosphonic acids," *Appl. Surf. Sci.*, vol. 416, pp. 716–724, 2017, doi: 10.1016/j.apsusc.2017.04.143.

[21] R. B. Merlet, M. A. Pizzoccaro-Zilamy, A. Nijmeijer, and L. Winnubst, "Hybrid ceramic membranes for organic solvent nanofiltration: State-of-the-art and challenges," *J. Memb. Sci.*, vol. 599, no. January, p. 117839, 2020, doi: 10.1016/j.memsci.2020.117839.

[22] J. Randon and R. Paterson, "Preliminary studies on the potential for gas separation by mesoporous ceramic oxide membranes surface modified by alkyl phosphonic acids," *J. Memb. Sci.*, vol. 134, no. 2, pp. 219–223, 1997, doi: 10.1016/S0376-7388(97)00110-5.

[23] H. B. He, Y. Q. Feng, Qu-Li, S. L. Da, and Z. X. Hu, "Preparation and evaluation of n-octadecylphosphonic acid-modified magnesia-zirconia stationary phases for reversed-phase liquid chromatography," *Anal. Chim. Acta*, vol. 542, no. 2, pp. 268–279, 2005, doi: 10.1016/j.aca.2005.04.010.

[24] J. Ding, Q. Gao, D. Luo, Z. G. Shi, and Y. Q. Feng, "n-Octadecylphosphonic acid grafted mesoporous magnetic nanoparticle: Preparation, characterization, and application in magnetic solid-phase extraction," *J. Chromatogr. A*, vol. 1217, no. 47, pp. 7351–7358, 2010, doi: 10.1016/j.chroma.2010.09.074.

[25] S. A. Paniagua *et al.*, "Phosphonic Acids for Interfacial Engineering of Transparent Conductive Oxides," *Chem. Rev.*, vol. 116, no. 12, pp. 7117–7158, 2016, doi: 10.1021/acs.chemrev.6b00061.

[26] F. Brodard-Severac, G. Guerrero, J. Maquet, P. Florian, C. Gervais, and P. H. Mutin, "High-field ^{17}O MAS NMR investigation of phosphonic acid monolayers on titania," *Chem. Mater.*, vol. 20, no. 16, pp. 5191–5196, 2008, doi: 10.1021/cm8012683.

[27] D. Geldof *et al.*, "Binding modes of phosphonic acid derivatives adsorbed on TiO_2 surfaces: Assignments of experimental IR and NMR spectra based on DFT/PBC calculations," *Surf. Sci.*, vol. 655, no. September 2016, pp. 31–38, 2017, doi:

10.1016/j.susc.2016.09.001.

[28] X. Chen, E. Luais, N. Darwish, S. Ciampi, P. Thordarson, and J. J. Gooding, “Studies on the effect of solvents on self-assembled monolayers formed from organophosphonic acids on indium tin oxide,” *Langmuir*, vol. 28, no. 25, pp. 9487–9495, 2012, doi: 10.1021/la3010129.

[29] G. A. Parks, “The isoelectric points of solid oxides, solid hydroxides, and aqueous hydroxo complex systems,” *Chem. Rev.*, vol. 65, no. 2, pp. 177–198, Apr. 1965, doi: 10.1021/cr60234a002.

[30] W. A. Schafer, P. W. Carr, E. F. Funkenbusch, and K. A. Parson, “Physical and chemical characterization of a porous phosphate-modified zirconia substrate,” *J. Chromatogr. A*, vol. 587, no. 2, pp. 137–147, 1991, doi: 10.1016/0021-9673(91)85150-E.

[31] C. Queffélec, M. Petit, P. Janvier, D. A. Knight, and B. Bujoli, “Surface modification using phosphonic acids and esters,” *Chem. Rev.*, vol. 112, no. 7, pp. 3777–3807, 2012, doi: 10.1021/cr2004212.

[32] D. Veclani, A. Melchior, A. Llobet, N. Armaroli, and A. Venturini, “Analysis of the role of the pH in the anchoring of alkylphosphonic acid on a TiO_2 surface: A DFTB study,” *Comput. Mater. Sci.*, vol. 219, no. December 2022, p. 111997, 2023, doi: 10.1016/j.commatsci.2022.111997.

[33] C. C. Aquino *et al.*, “Amine-functionalized titania-based porous structures for carbon dioxide postcombustion capture,” *J. Phys. Chem. C*, vol. 117, no. 19, pp. 9747–9757, 2013, doi: 10.1021/jp312118e.

[34] G. A. Seisenbaeva *et al.*, “Molecular insight into the mode-of-action of phosphonate monolayers as active functions of hybrid metal oxide adsorbents. Case study in sequestration of rare earth elements,” *RSC Adv.*, vol. 5, no. 31, pp. 24575–24585, 2015, doi: 10.1039/C4RA15531A.

[35] P. Li *et al.*, “In-situ preparation of amino-terminated dendrimers on TiO_2 films by generational growth for potential and efficient surface functionalization,” *Appl. Surf. Sci.*, vol. 459, no. April, pp. 438–445, 2018, doi: 10.1016/j.apsusc.2018.08.044.

[36] P. Canepa, G. Gonella, G. Pinto, V. Grachev, M. Canepa, and O. Cavalleri, “Anchoring

of Aminophosphonates on Titanium Oxide for Biomolecular Coupling," *J. Phys. Chem. C*, vol. 123, no. 27, pp. 16843–16850, 2019, doi: 10.1021/acs.jpcc.9b04077.

[37] N. Gys *et al.*, "Experimental and computational insights into the aminopropylphosphonic acid modification of mesoporous TiO_2 powder: The role of the amine functionality on the surface interaction and coordination," *Appl. Surf. Sci.*, vol. 566, no. December 2020, p. 150625, 2021, doi: 10.1016/j.apsusc.2021.150625.

[38] N. Gys *et al.*, "Amino-Alkylphosphonate-Grafted TiO_2: How the Alkyl Chain Length Impacts the Surface Properties and the Adsorption Efficiency for Pd," *ACS Omega*, vol. 7, no. 49, pp. 45409–45421, Dec. 2022, doi: 10.1021/acsomega.2c06020.

[39] C. Tudisco, V. Oliveri, M. Cantarella, G. Vecchio, and G. G. Condorelli, "Cyclodextrin anchoring on magnetic Fe_3O_4 nanoparticles modified with phosphonic linkers," *Eur. J. Inorg. Chem.*, no. 32, pp. 5323–5331, 2012, doi: 10.1002/ejic.201200510.

[40] J. G. Van Dijck *et al.*, "Synthesis – properties correlation and the unexpected role of the titania support on the Grignard surface modification," *Appl. Surf. Sci.*, vol. 527, no. January, 2020, doi: 10.1016/j.apsusc.2020.146851.

[41] N. Gys *et al.*, "Self-Induced and Progressive Photo-Oxidation of Organophosphonic Acid Grafted Titanium Dioxide," *Chempluschem*, vol. 88, no. 3, p. e202200441, Mar. 2023, doi: https://doi.org/10.1002/cplu.202200441.

[42] L. S. Dake and R. J. Lad, "Ultrathin Al Overlayers on Clean and K-Covered TiO_2 (110) Surfaces," *Surf. Sci. Spectra*, vol. 4, no. 3, pp. 232–245, 1996, doi: 10.1116/1.1247823.

[43] P. Giannozzi *et al.*, "QUANTUM ESPRESSO: A modular and open-source software project for quantum simulations of materials," *J. Phys. Condens. Matter*, vol. 21, no. 39, 2009, doi: 10.1088/0953-8984/21/39/395502.

[44] P. Giannozzi *et al.*, "Advanced capabilities for materials modelling with Quantum ESPRESSO," *J. Phys. Condens. Matter*, vol. 29, no. 46, p. 465901, 2017, doi: 10.1088/1361-648X/aa8f79.

[45] P. Giannozzi *et al.*, "Quantum ESPRESSO toward the exascale," *J. Chem. Phys.*, vol. 152, no. 15, p. 154105, Apr. 2020, doi: 10.1063/5.0005082.

[46] Z. Wu and R. E. Cohen, "More accurate generalized gradient approximation for solids,"

Phys. Rev. B - Condens. Matter Mater. Phys., vol. 73, no. 23, pp. 2–7, 2006, doi: 10.1103/PhysRevB.73.235116.

[47] F. Tran, R. Laskowski, P. Blaha, and K. Schwarz, "Performance on molecules, surfaces, and solids of the Wu-Cohen GGA exchange-correlation energy functional," *Phys. Rev. B - Condens. Matter Mater. Phys.*, vol. 75, no. 11, pp. 1–14, 2007, doi: 10.1103/PhysRevB.75.115131.

[48] P. E. Blöchl, "Projector augmented-wave method," *Phys. Rev. B*, vol. 50, no. 24, pp. 17953–17979, 1994, doi: 10.1103/PhysRevB.50.17953.

[49] S. Grimme, "Semiempirical GGA-Type Density Functional Constructed with a Long-Range Dispersion Correction," *J. Comput. Chem.*, vol. 32, pp. 174–182, 2006, doi: 10.1002/jcc.

[50] V. Barone, "Role and Effective Treatment of Dispersive Forces in Materials: Polyethylene and Graphite Crystals as Test Cases," *J. Comput. Chem.*, vol. 32, pp. 174–182, 2009, doi: 10.1002/jcc.

[51] M. Lazzeri, A. Vittadini, and A. Selloni, "Structure and energetics of stoichiometric TiO_2 anatase surfaces," *Phys. Rev. B - Condens. Matter Mater. Phys.*, vol. 63, no. 15, pp. 1554091–1554099, 2001, doi: 10.1103/PhysRevB.63.155409.

[52] G. Liu, H. G. Yang, J. Pan, Y. Q. Yang, G. Q. M. Lu, and H. M. Cheng, "Titanium dioxide crystals with tailored facets," *Chem. Rev.*, vol. 114, no. 19, pp. 9559–9612, 2014, doi: 10.1021/cr400621z.

[53] L. Mino, G. Spoto, S. Bordiga, and A. Zecchina, "Particles morphology and surface properties as investigated by HRTEM, FTIR, and periodic DFT calculations: From pyrogenic TiO_2 (P25) to nanoanatase," *J. Phys. Chem. C*, vol. 116, no. 32, pp. 17008–17018, 2012, doi: 10.1021/jp303942h.

[54] T. Björkman, "CIF2Cell: Generating geometries for electronic structure programs," *Comput. Phys. Commun.*, vol. 182, no. 5, pp. 1183–1186, 2011, doi: 10.1016/j.cpc.2011.01.013.

[55] C. J. Pickard and F. Mauri, "All-electron magnetic response with pseudopotentials: NMR chemical shifts," *Phys. Rev. B - Condens. Matter Mater. Phys.*, vol. 63, no. 24, pp.

2451011–2451013, 2001, doi: 10.1103/physrevb.63.245101.

[56] D. Müller, E. Jahn, G. Ladwig, and U. Haubenreisser, "High-resolution solid-state ^{27}Al and ^{31}P NMR: correlation between chemical shift and mean Al-O-P angle in $AlPO_4$ polymorphs," *Chem. Phys. Lett.*, vol. 109, no. 4, pp. 332–336, 1984, doi: 10.1016/0009-2614(84)85596-7.

[57] K. Momma and F. Izumi, "VESTA3 for three-dimensional visualization of crystal, volumetric and morphology data," *J. Appl. Crystallogr.*, vol. 44, no. 6, pp. 1272–1276, 2011, doi: 10.1107/S0021889811038970.

[58] M. D. Losego, J. T. Guske, A. Efremenko, J. P. Maria, and S. Franzen, "Characterizing the molecular order of phosphonic acid self-assembled monolayers on indium tin oxide surfaces," *Langmuir*, vol. 27, no. 19, pp. 11883–11888, 2011, doi: 10.1021/la201161q.

[59] D. M. Spori, N. V. Venkataraman, S. G. P. Tosatti, F. Durmaz, N. D. Spencer, and S. Zürcher, "Influence of alkyl chain length on phosphate self-assembled monolayers," *Langmuir*, vol. 23, no. 15, pp. 8053–8060, 2007, doi: 10.1021/la700474v.

[60] M. Kosmulski, "The significance of the difference in the point of zero charge between rutile and anatase," *Adv. Colloid Interface Sci.*, vol. 99, no. 3, pp. 255–264, 2002, doi: 10.1016/S0001-8686(02)00080-5.

[61] C. E. McNamee, Y. Tsujii, and M. Matsumoto, "Physicochemical characterization of an anatase TiO_2 surface and the adsorption of a nonionic surfactant: An atomic force microscopy study," *Langmuir*, vol. 21, no. 24. pp. 11283–11288, 2005, doi: 10.1021/la0517890.

[62] J. W. Bullard and M. J. Cima, "Orientation dependence of the isoelectric point of TiO_2 (rutile) surfaces," *Langmuir*, vol. 22, no. 24, pp. 10264–10271, 2006, doi: 10.1021/la061900h.

[63] P. C. Crofts and G. M. Kosolapoff, "Preparation and Determination of Apparent Dissociation Constants of Some Alkylphosphonic and Dialkylphosphinic Acids," *J. Am. Chem. Soc.*, vol. 75, no. 14, pp. 3379–3383, 1953, doi: 10.1021/ja01110a024.

[64] L. D. Freedman and G. O. Doak, "The Preparation and Properties of Phosphonic Acids," *Chem. Rev.*, vol. 57, no. 3, pp. 479–523, 1957, doi: 10.1021/cr50015a003.

[65] Z. Chen, W. He, M. Beer, M. Megharaj, and R. Naidu, “Speciation of glyphosate, phosphate and aminomethylphosphonic acid in soil extracts by ion chromatography with inductively coupled plasma mass spectrometry with an octopole reaction system,” *Talanta*, vol. 78, no. 3, pp. 852–856, 2009, doi: 10.1016/j.talanta.2008.12.052.

[66] G. W. Gokel, *Dean’s Handbook Of Organic Chemistry, 2nd Edition*. McGraw-Hill, 2004.

[67] Q. Nguyen Thi, “Development of hybrid photoelectrodes via assemblage of a ruthenium based photosensitizer and a metal-metal oxide nanocatalyst for the solar O_2 generation,” Université Paul Sabatier - Toulouse III, 2021.

[68] A. Hemeryck, A. Motta, C. Lacaze-Dufaure, D. Costa, and P. Marcus, “DFT-D study of adsorption of diaminoethane and propylamine molecules on anatase (101) TiO_2 surface,” *Appl. Surf. Sci.*, vol. 426, pp. 107–115, 2017, doi: 10.1016/j.apsusc.2017.07.161.

[69] S. Brunauer, P. H. Emmett, and E. Teller, “Adsorption of Gases in Multimolecular Layers,” *J. Am. Chem. Soc.*, vol. 60, no. 2, pp. 309–319, 1938, doi: 10.1021/ja01269a023.

[70] M. Thommes *et al.*, “Physisorption of gases , with special reference to the evaluation of surface area and pore size distribution (IUPAC Technical Report),” 2015, doi: 10.1515/pac-2014-1117.

[71] U. Diebold, N. Ruzycki, G. S. Herman, and A. Selloni, “One step towards bridging the materials gap: Surface studies of TiO_2 anatase,” *Catal. Today*, vol. 85, no. 2–4, pp. 93–100, 2003, doi: 10.1016/S0920-5861(03)00378-X.

[72] L. Mino *et al.*, “Beyond Shape Engineering of TiO_2 Nanoparticles: Post-Synthesis Treatment Dependence of Surface Hydration, Hydroxylation, Lewis Acidity and Photocatalytic Activity of TiO_2 Anatase Nanoparticles with Dominant {001} or {101} Facets,” *ACS Appl. Nano Mater.*, vol. 1, no. 9, pp. 5355–5365, 2018, doi: 10.1021/acsanm.8b01477.